Study on Formation Condition of Cometary Ice on the Basis of Ortho-to-Para Ratio of Ammonia

Hideyo Kawakita

DOCTOR OF SCIENCE

Department of Astronomical Science School
of Mathematical and Physical Science
The Graduate University for Advanced Studies

2001

Contents

List of Figures

List of Tables

Abstract

Comets are thought to be relics of our solar system, which have kept the information on solar system formation. The solar system formed from a collapsing molecular cloud. Many planetesimals formed first in the proto-planetary disk around proto-Sun (called "solar nebula"). Typical dimensions of the planetesimals were between a few hundreds meters and a few kilometers. They accreted into planets and satellites, while some of them remained as fragments of collisions which are asteroids, and the remnants of icy planetesimals survived in outer solar system as comets or small icy bodies. Therefore, studies on physical conditions of the solar nebula from a viewpoint of comets are important for investigating the formation process or circumstance of the solar system.

There are some primordial properties in comets, e.g, a chemical abundance, isotopic ratios for various elements, and ortho-to-para ratios (OPRs) of cometary materials. The OPR is an important character of cometary molecules which have hydrogen atoms at symmetrical positions. A spin temperature derived from OPR could reflect the conditions (especially, a temperature) where the molecule formed. The spin temperature is thought to indicate a temperature of grains in the solar nebula because the molecules formed in the icy mantles on grains.

Among cometary species there are no reliable reports except water molecules, of which the spin temperature has been derived as about 30 K for several comets. This temperature is consistent with the temperature range investigated from deuterium-to-hydrogen (D/H) ratios of water and hydrogen cyanide, and from abundances of argon and neon in comets. In this thesis, a new method to investigate OPR of ammonia in comets, along with first applications of this method to two Oort cloud comets, comet C/1999S4 (LINEAR) and comet C/2001A2 (LINEAR), is presented. Ammonia is important as a product of nitrogen related chemical reactions in the solar nebula, and as a reservoir of nitrogen atoms in comets. However, there are only a few reports on the detection of cometary ammonia for bright comets by radio observations, and no reports on OPR of cometary ammonia.

In this thesis, it is shown that the OPR of cometary ammonia can be also

determined from OPR of NH_2, which is observable in the optical wavelength region. NH_2 is thought to be a photodissociation product of cometary ammonia, which is confirmed by the spatial distribution of NH_2 in the coma of comet C/1996B2 (Hyakutake). In order to derive the OPR of NH_2 from observed emission lines, the fluorescence excitation model is established. As an application of this model to the high-dispersion optical spectra taken by the high dispersion spectrograph (HDS) and the Subaru telescope, the OPRs of NH_2 are derived as 3.32±0.09 in comet C/1999S4 (LINEAR) and as 3.43±0.09 in comet C/2001A2 (LINEAR), respectively. These values indicate OPRs of ammonia to be 1.16±0.05 and 1.22±0.05 for comet C/1999S4 (LINEAR) and comet C/2001A2 (LINEAR), respectively.

Derived spin temperatures of ammonia, 28^{+3}_{-2} K for comet C/1999S4 (LINEAR) and 26^{+2}_{-1} K for comet C/2001A2 (LINEAR), are consistent with temperature ranges investigated for the Oort cloud comets in the previous studies. These results are indicative of grain processing for the formation of cometary ammonia. The derived spin temperatures may indicate the formation region between the orbit of Saturn to that of Uranus in the solar nebula. These comets are thought to originate from Oort cloud concerning their orbits. Based on statistical studies on orbital evolutions of comets in the solar nebula, it is thought that Oort cloud comets formed between the orbits of Jupiter and Neptune and then they were scattered by giant planets into outer edge of the solar system. The result obtained in this study is consistent with the statistical studies on orbital evolution of the Oort cloud comets.

Further observations of OPR of cometary ammonia are required, especially, a comparison between Oort cloud comets and Kuiper belt comets (which are thought to form further than the orbit of Neptune in the solar nebula) is important for investigating origin of comets.

Chapter 1

General Introduction

Comet is a remnant of solar nebula (a protoplanetary disk around proto-Sun) and it has kept the information on early solar system. Physical conditions such as a temperature, a pressure, and a chemical composition of our solar nebula, can be investigated from comets. Studies on formation process of our solar system are important for investigations on the formation of stars and planetary systems. Many stars with planets and the protoplanetary disks around protostars have been discovered so far and the formation process from a molecular cloud to a planetary system has been investigated by many researchers (Shu et al. 1987, Marcy et al. 2000, Aikawa et al. 2001, Irvine et al. 2000, and references therein).

In the solar nebula which consisted of gas and dust grains, many planetesimals formed from grains (or grains with icy mantles) at near equatorial plane of solar nebula, and a typical size of planetesimals is thought to be between a few hundreds meters and a few kilometers (cf. Crovisier & Encrenaz 2000). These gas and dust grains originated from a pre-solar molecular cloud. The planetesimals accreted into several planets and their satellites in the solar system. Comets are thought to be remnants of icy planetesimals formed apart from the central proto-Sun, and they have survived until now in the solar system. Therefore, the chemical composition of a comet reflects the chemical composition and physical conditions in the solar nebula, especially in the outer region. These remnants have been reserved in the outer part of solar system for a long time ($\approx$ 4.5 Gyr). One reservoir is "Oort cloud" spherically distributed between 10^4 and 10^5 astronomical units (AU) from the Sun, and the other is "Edgeworth-Kuiper belt" (hereafter called "Kuiper belt" briefly) distributed beyond 30 AU from the Sun nearly in the equatorial plane of the solar system (Weissman 1999, Trujillo & Brown 2001).

Usually comets come from these regions and form comae and tails due to the solar irradiation within a few AU from the Sun (cf. Crovisier & Encrenaz 2000). The coma spherically distributed around cometary nucleus,

consists of both gaseous volatile species sublimated from the nucleus, and dust grains ejected from the nucleus by an expanding gas flow. Some kinds of molecules or atoms are generated through photodissociations of cometary molecules by the solar ultraviolet radiation and through chemical reactions in the coma (chemical reactions can occur only in the inner coma because the gas density is too low in the outer coma). There are three types of cometary tails: a dust tail, an ion tail, and a sodium tail. The dust tail consists of dust grains which are ejected from the cometary nucleus by the expanding gas flow and accelerated by the solar radiation pressure. The ion tail is formed by ions which are generated from neutral molecules in the coma and accelerated by the solar wind. The sodium tail is made from neutral sodium atoms which are accelerated by solar radiation pressure (the atomic sodium is very sensitive to the solar radiation). The sodium tail is discovered only in several bright comets (Cremonese 1999, Kawakita & Fujii 1998, Combi et al. 1997a).

Thus the materials of which a cometary nucleus consists can be easily observed within a few AU from the Sun. Recent progress of modeling a chemical evolution in a protoplanetary disk and in a molecular cloud can allow us to relate the chemical composition of our solar nebula to those of cometary nuclei. A chemical evolution in the protoplanetary disk is sensitive to the temperature and other conditions (Aikawa et al. 1999). A chemical abundance in cometary nucleus seems to be similar to that in molecular clouds for some comets (Bockelée-Morvan et al. 2000). It is thought that some materials might be incorporated into comets from a molecular cloud without processing in the solar nebula. The deuterium fractionation in cometary materials, e.g., water, hydrogen cyanide and etc., is also important key for the study on chemical evolution in the solar nebula. The deuterium-to-hydrogen ratio (D/H ratio) is sensitive to the conditions of solar nebula (Hersant et al. 2001, Aikawa & Herbst 1999). Of course, other isotopic species are also important. The isotopic ratios in carbon, oxygen, nitrogen, and sulfur are consistent with the solar abundance, and this fact supports that the comets originated from the solar nebula (Crovisier 1999).

Oh the other hand, the ortho-to-para ratio (OPR) of a cometary material is also an important key to investigate the temperature of solar nebula. For a molecule with hydrogen atoms at symmetrical positions, there are different nuclear-spin species according to the relative orientations of the spins of their protons. A situation is the same for a molecule with identical

atoms having non-zero nuclear spin at symmetrical positions. These species are called "ortho" and "para" for molecules with two identical protons like H_2O, "A" and "E" (or "A", "E", and "F") for molecules with three (or four) identical protons. It is thought that the OPR (or E/A ratio) of the molecules is characteristic of the formation conditions of the molecules and it is one of primordial characters of comets (Mumma et al. 1993, Crovisier 1999, Irvine 1999) even though the possibility of ortho-para conversion in the cometary environment can not be avoided and should be investigated in the laboratory (Irvine et al. 2000).

Unfortunately, there are no reliable reports on OPR of cometary molecules except water (Mumma et al. 1993, Crovisier 1999). Although Biver et al. (1999) reported OPR of formaldehyde (H_2CO) in comet C/1996B2 (Hyakutake), they noted that readers must be very careful for their result because the calibration uncertainties were large due to low atmospheric transmission for para-H_2CO lines. As preliminary reports, Weaver et al. (1997) reported E/A ratio of methane (CH_4) in comet C/1996B2 (Hyakutake), and Womack et al. (1997) reported OPR of formaldehyde in comet C/1995O1 (Hale-Bopp). However, there are no further reports for them in detail.

Although ammonia is important as a product of nitrogen related chemical reactions in solar nebula and as a reservoir of nitrogen atoms in comets, there are no reports on OPR of cometary ammonia so far. In this thesis cometary ammonia is investigated from a viewpoint of its ortho-to-para ratio (the nuclear-spin species of ammonia are usually called "ortho" and "para" although ammonia molecule has three identical protons). Ammonia with $K = 3n$ (K: a quantum number of total angular momentum projected to its molecular symmetric axis, and n is an integer) is called "ortho" and the other is called "para" (Ho & Townes 1983). Because it is difficult to determine the precise OPR of cometary ammonia directly from observations of ammonia as described in Chapter 4, NH_2 is used to probe the OPR of cometary ammonia in this thesis. Cometary ammonia is photodissociated by solar ultraviolet radiation in the cometary coma and makes NH_2 and H atom. NH_2 has two identical hydrogen atoms and there are "ortho" and "para" species for NH_2. The OPR of NH_2 depends on the OPR of ammonia. Thus the OPR of ammonia can be investigated from NH_2 indirectly. The most important advantage of using NH_2 is that NH_2 is usually seen in optical spectra of comets near 1 AU from the Sun, and a high signal-to-noise (S/N) ratio can be achieved for NH_2 emission lines. On

the other hand, cometary ammonia could be detected only for a few bright comets using existing facilities. These advantages make it easy to observe many comets and to determine the OPR of ammonia in the comets. In the future, a statistical study on OPR of cometary ammonia in various comets will be possible based on the method provided in this thesis. It is important for investigating the history of our solar system. The main purposes of this thesis are to establish a new tool to investigate the OPR of cometary ammonia and to introduce the first application of this method to two comets.

In Chapter 2, the spatial distribution of NH_2 in comet C/1996B2 (Hyakutake) is compared with model results based on the Monte Carlo simulation, in order to confirm that ammonia is a parent of NH_2 in comets.

In Chapter 3, the fluorescence excitation model of cometary NH_2 is constructed and the model results are shown. This model is necessary to determine the OPR of NH_2 from a high-dispersion spectrum of comet. The model results are discussed and compared with observational results.

In Chapter 4, OPRs of NH_2 are determined from the observed NH_2 emission spectra of comet C/1999S4 (LINEAR) and comet C/2001A2 (LINEAR). Then OPRs of cometary ammonia are determined from the OPRs of NH_2 for these comets. The derived OPRs of ammonia in these comets are discussed and compared with other observations.

Chapter 2

Confirmation of NH_2 Production through Photodissociation of Ammonia

2.1 Introduction

Recently there are two comets which got very closer to the Earth before comet C/1996B2 (Hyakutake), these comets are comet C/1983H1 (IRAS-Araki-Alcock) hereafter called comet IAA, and comet C/1983J1 (Sugano-Saigusa-Fujikawa) hereafter called comet SSF. The researchers had the best opportunities to observe the condition near the cometary nuclei in detail for these comets. Comet IAA approached to the Earth up to $\Delta = 0.03$ AU in May 1983, and comet SSF approached to the Earth up to $\Delta = 0.06$ AU in June 1983. Several new molecules were discovered at these comets via UV, visible, infra-red and radio observations. Especially via radio observations, some saturated molecules were discovered, which are thought to be released from the nucleus directly.

The emission of NH_2 molecule caused by the photodissociation is shown in the visible region from about 4000 Å to 9000 Å. Because these features are, however, faint and contaminated with the other strong emission such as the C_2 Swan band sequence, the number of the researches on the NH_2 molecules is relatively small. Furthermore, the surface brightness profile near the nucleus (at some NH_2 emission band) should be used to determine the lifetime of NH_2 parent molecule precisely. The spatial resolution should be less than 10^3 km because the scale length of NH_2 parent based on Haser's model is about the same order. For comet IAA and SSF, however, it was difficult to get high quality data (which has high S/N ratio and low tracking error). The reasons were as follows; (1) the comets were diffused and faint (especially for comet SSF), (2) because of its rapid motion it was difficult to track the comet during sufficient exposure time (especially for

comet IAA), (3) the CCD devices were not well developed at that time, so longer exposure time was required for the photographic observation and the accuracy of the photographic photometry is less than the CCD photometry.

On the other hand, comet C/1996B2 (Hyakutake) became bright and CCD devices were well developed at that time, so it was not hard to obtain excellent data in spite of its rapid motion. Comet C/1996B2 (Hyakutake) approached to the Earth up to 0.10 AU in March 1996. The spectroscopic observations in the visible region were performed using the long slit spectrograph on 1996 March 23, and 1-dimensional profile of the brightness was obtained at the wavelength of NH_2 emission. The spatial resolution of the observations was about 645 km and this value is sufficient to check the lifetime of its parent molecule. The most reliable candidate of the NH_2 parent molecule is the ammonia (NH_3), which was securely detected for the first time in comet C/1996B2 (Hyakutake) by radio observations (Bird et al. 1997b). In this study, three possible parent of NH_2 radicals (including NH_3) are examined by comparing the observed surface brightness profile with the calculations based on the collisional random walk model.

2.2 Observation of Comet C/1996B2 (Hyakutake)

The result in this chapter is derived from the observations carried out by 1.01m reflector (F/12, Folded-Cassegrain focus) at Bisei Astronomical Observatory (BAO), Okayama, Japan. The low-dispersion grating spectrometer (the spectral resolution; FWHM = 12 Å) was used with electronic cooled CCD camera (ST-6, SBIG). The slit size is 25 mm $\times$120 μm, corresponding to 425 arcsec $\times$2 arcsec on the celestial sphere. The spatial resolution is 1.9 arcsec pixel^{-1} on the CCD chip.

Comet C/1996B2 (Hyakutake) was observed on 1996 March 23 (UT), the heliocentric distance and the geocentric distance of the comet were 1.074 AU and 0.113 AU at the time, respectively. The slit was put on the optical center of the coma, with the direction of north-south-ward. This comet moved rapidly at the time because it was close to the Earth. The telescope tracked automatically the comet during an exposure, the tracking error for the comet is within 5 arcsec. The spatial resolution (including the tracking error and the seeing size) is estimated to be about 645 km at the comet. The spectrophotometric standard star (HR5191) was also observed in order to correct for variations of instrumental sensitivity at the different wavelengths used in the comet observation.

To reduce and analyze the observations NOAO IRAF (Image Reduction and Analysis Facility) software was used in this paper. The raw spectrum image was bias-subtracted, and flat-fielded at the first, then the sky frame was subtracted from the object frame. After sky-subtraction, the signal from the comet (emission + continuum) was divided by the instrumental sensitivity function which was determined from the spectrum of the spectrophotometric standard star.

Figure 2.1 shows the obtained spectrum, where several emission features of NH_2, i.e. NH_2(0,7,0), (0,8,0) and (0,9,0) bands are recognized. These features are weak relative to other strong emissions such as C_2 Swan band. NH_2(0,9,0) is contaminated with $C_2(\Delta v = -2)$ band (Brown et al. 1996). Although NH_2(0,8,0) band is also contaminated with [OI] (at 6300 Å and 6364 Å), the pure NH_2 emission between these [OI] lines can be extracted because NH_2(0,8,0) band has a peak at 6334 Å. So the NH_2(0,8,0) band was measured as the surface brightness profile of NH_2 emission. Finally, the continuum level at the NH_2(0,8,0) band emission was linearly interpolated using neighbor continuum levels (at 6250 Å and 6400 Å), and was subtracted from the brightness profile. Thus, the NH_2(0,8,0) band spatial profile was obtained.

2.3 Haser's Model Analysis

As a preliminary analysis, the profile calculated by Haser's model has been fitted to the obtained profile. The scale lengths used here, $\lambda_d = 5.10 \times 10^4$ km for a daughter and $\lambda_p = 4.03 \times 10^3$ km for a parent at the observation, are consistent with the typical scale lengths for NH_2 (Fink & Hicks 1996). Figure 2.2 shows obtained NH_2 profile, the calculation based on Haser's model and the point spread function (PSF) representing the spatial error. The error bars of the surface brightness profile were estimated by the following manner. At first, the profile of difference between the original surface brightness profile and the profile which was moving averaged (the window size is 5 pixel) was calculated. The standard deviation of points within the local section is nearly constant everywhere on the slit for the differential profile, so the standard deviation for all points along the slit is calculated and shown in the Figure 2.2 as the error bars. In Figure 2.2, it is found that the data where the nucleocentric distance is less than $10^{5.5}$ m should be ignored because of the PSF (a half of FWHM of PSF is nearly equal to $10^{5.5}$ m).

Table 2.1: Observational parameters for C/1996B2 (Hyakutake)

Object	Date	Time	Exp. Time
HR5191	1996 Mar 23	17:30(UT)	3 s × 3
C/1996B2 (Hyakutake)	1996 Mar 23	18:40(UT)	60 s × 3
Sky	1996 Mar 23	19:02(UT)	60 s × 2

However, because the density of the molecules is high in the inner coma so that the mean free path of the molecule is shorter relative to the typical scale considered (which is the slit length in this case), the effect of the collisions between the molecules should not be neglected in this case. The Haser's model can not deal with this collisional effect. The collision zone radius, r_c, is defined as the nucleocentric distance at which the path length between collisions is equal to the nucleocentric distance, and this is represented by

$$r_c = \frac{Q\sigma}{4\pi v}, \tag{2.1}$$

where Q denotes the water production rate, σ denotes the collision cross section and v denotes the gas outflow velocity (Tegler et al. 1992). The water production rate, $Q(H_2O)$, was determined directly from the emission of H_2O in the infra-red region on 1996 March 23; $Q(H_2O) = 1.5 \times 10^{29}$ molecules s^{-1} by Mumma et al. (1996). Tegler et al. (1992) used $\sigma = 5.0 \times 10^{-25}$ km^2 for H_2O-H_2O collisions and $v = 1.0$ km s^{-1}. These values and above equation give $r_c = 6.0 \times 10^3$ km, so about 1/3 of the slit length corresponds to the collisional zone (used slit length is 3.24×10^4 km). Clearly the collisional effect can not be neglected in the calculation. Although the result of Haser's model fitting shown in Figure 2.2 seems to be good at a glance, other model which can deal with the collisional effect to determine the lifetime of NH_2 and its parent must be taken here.

2.4 Collisional Random Walk Model for Inner Coma

Not only Haser's model but also the vectorial model (which is more realistic than Haser's model, Festou 1981) can not deal with the collisions between molecules, these models can be applied only out of collisional sphere. For the analysis of the data, the random walk model which is based on the

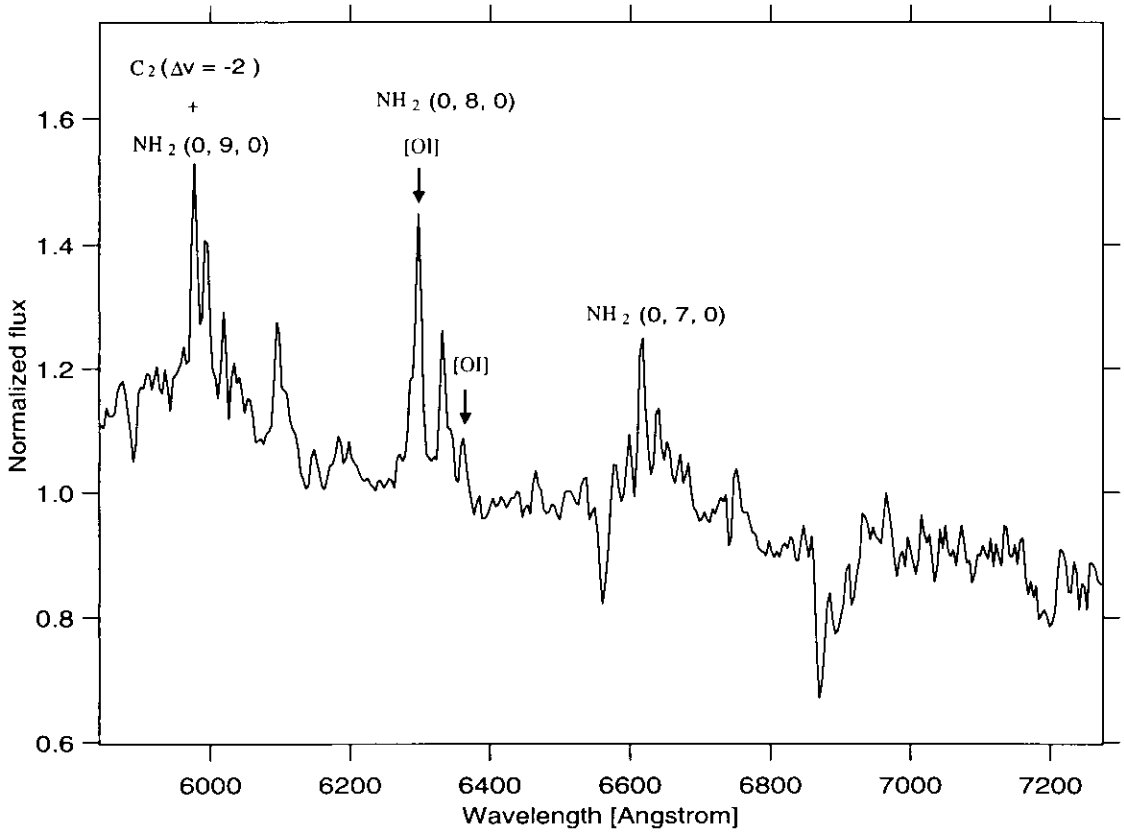

Figure 2.1: The spectrum of comet C/1996B2 (Hyakutake) observed on 1996 March 23.8 (UT). The flux is normalized to unity at the 6250 Å continuum level. $C_2(\Delta v = -2)$, NH_2 emissions and forbidden line of oxygen atom are shown.

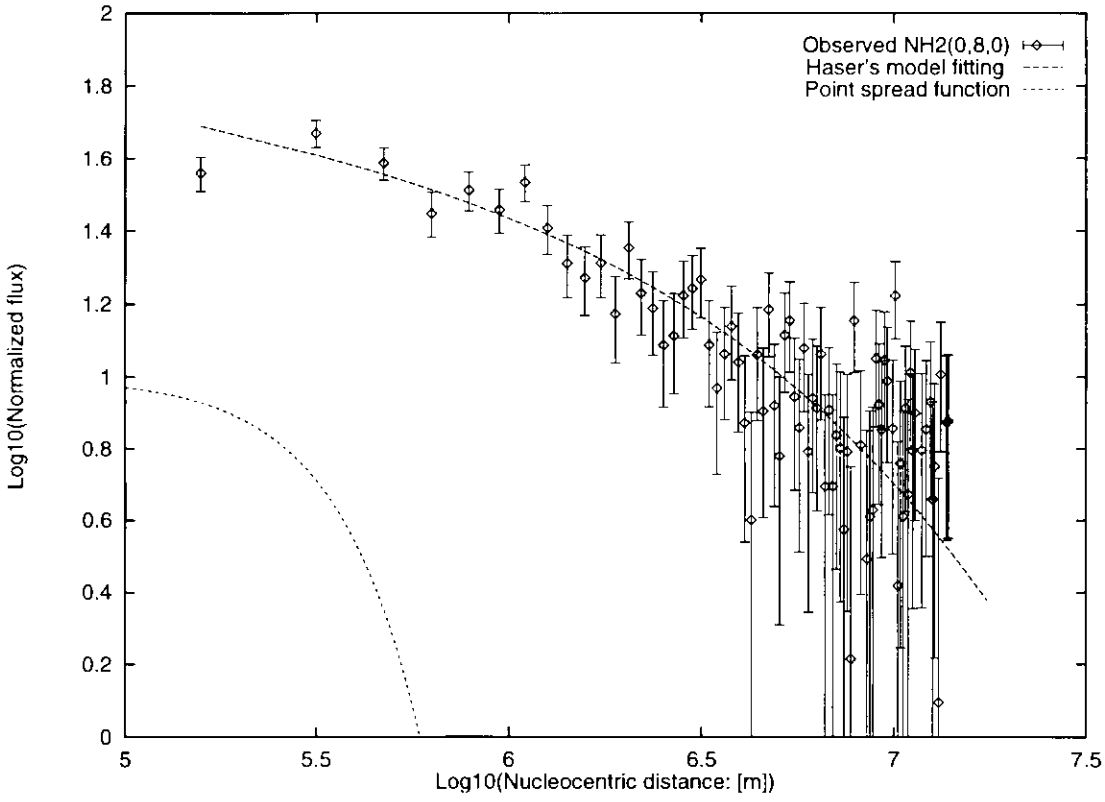

Figure 2.2: The surface brightness profile of $NH_2(0,8,0)$, where the error-bars indicate 1σ error level. The dashed line is calculated by Haser's model (see text). The dotted line indicates the point spread function in this case.

Monte Carlo simulation (Combi & Delsemme 1980) is taken here. In this model the collisions can be dealt with easily. However, many particles enough to achieve a quasi steady-state (10^6 particles in this paper) must be traced, so it takes to calculate for a long time relative to Haser's model. The collisional random walk model presented here is based on the model presented by Tegler et al. (1992). In the model it is assumed that the parent of NH_2 is NH_3 and NH_3 is released from the nucleus directly, and most of parameters necessary for the model are also referred from Tegler et al. (1992). The other NH_2 parent molecules are also shown in the later part.

Consider a time interval of length T_F, which start is represented as $t = 0$ and the end of the interval is represented as $t = T_F$. The parent molecule, NH_3, is released at t = t_i ($0 \leq t_i < T_F$), which is given by random number between 0 and 1; R_i and

$$t_i = R_i T_F. \tag{2.2}$$

The velocity of released NH_3 is given as the vector sum of the radial bulk outflow velocity and the randomized thermal component. The bulk outflow velocity has the direction which is specified by spherical polar angles, ϕ_i and θ_i, with origin at the nucleus of the comet. These angles are given by new random numbers ($R_{i,\phi}$ and $R_{i,\theta}$),

$$\phi_i = 2\pi R_{i,\phi} \tag{2.3}$$

and

$$\cos\theta_i = 1 - 2R_{i,\theta}. \tag{2.4}$$

The bulk outflow velocity is assumed to be $v = 1.0 \times r^{-0.5}$ km s^{-1} (Wyckoff et al. 1988, Tegler et al. 1992). The thermal velocity component has randomized direction and it is assumed its velocity distribution is given by the Maxwell-Boltzmann velocity distribution. A temperature of outflow coma is $T = 30$ K at 1 AU here (Hodges 1990).

The released parent molecule, NH_3, photodissociates at time $(t_i + t_{NH_3})$ and t_{NH_3} is given by

$$t_{NH_3} = \tau_{NH_3} r^2 \log(R_{NH_3}), \tag{2.5}$$

where τ_{NH_3} denotes the photodissociation time scale of NH_3 at 1 AU, r denotes comet's heliocentric distance and R_{NH_3} is new random number.

The photodissociation time scale, $\tau_{NH_3} = 7.7 \times 10^3$ s at 1 AU is assumed here (Tegler et al. 1992).

The UV photon gives the photodissociation energy to the NH_3 molecule, and NH_3 photodissociates into NH_2 and H. The excess of the photon energy over the photodissociation energy is imparted to the internal degrees of freedom of the NH_2 molecule and the additional kinetic energy. The velocity of NH_2 is given as the vector sum of the velocity of NH_3 and the additional velocity caused by the excess of energy. This additional velocity is assumed to be 0.8 km s^{-1} and its direction is randomized (Tegler et al. 1992).

The NH_2 molecule also photodissociates at time $(t_i + t_{NH_3} + t_{NH_2})$, and t_{NH_2} is given by

$$t_{NH_2} = \tau_{NH_2} r^2 \log(R_{NH_2}), \tag{2.6}$$

where τ_{NH_2} denotes the photodissociation time scale of NH_2 at 1 AU and R_{NH_2} is new random number. The photodissociation time scale, $\tau_{NH_2} = 3.3 \times 10^4$ s at 1 AU is assumed here (Tegler et al. 1992).

The collisions between the particle (NH_3 or NH_2) and the background out-flowing coma gas has also been considered. The elastic molecule-molecule collisions are assumed here. The dimensionless collision path length; $\lambda(= l/r_0)$, where l denotes the collision path length for a trajectory starting at a nucleocentric distance r_0, is determined from the following integral equation and new random number R_i (Combi et al. 1993);

$$-\ln(1-R_i) = \frac{Q\sigma}{4\pi v r_0 \gamma} \times \int_0^{\lambda} \frac{v_{\lambda'}[\mathrm{erf}(v_{\lambda'})(1 + 1/(2v_{\lambda'}^2)) + \exp(-v_{\lambda'}^2)/(\pi^{1/2} v_{\lambda'})]}{1 + 2\lambda' \cos\Theta + \lambda'^2} d\lambda', \tag{2.7}$$

where

$$v_{\lambda'} = \gamma[1 - 2\beta \frac{\lambda' + \cos\Theta}{(1 + 2\lambda' \cos\Theta + \lambda'^2)^{1/2}} + \beta^2]^{1/2}, \tag{2.8}$$

$$\alpha = \frac{m}{2kT}, \tag{2.9}$$

$$\beta = \frac{v}{u}, \tag{2.10}$$

$$\gamma = u\alpha^{1/2}. \tag{2.11}$$

Table 2.2: Lifetimes and ejection velocities for three possible parents of NH_2. These values are referred from Krasnopolsky & Tkachuk (1991) except the lifetime of ammonia, which is referred from Tegler et al. (1992).

Parent	Lifetime	Ejection velocity
NH_3	7.7×10^3 s	0.8 km s^{-1}
N_2H_4	2.7×10^3 s	1.6 km s^{-1}
CH_3NH_2	3.8×10^3 s	1.8 km s^{-1}

In above equations, Θ denotes a particle direction angle relative to outward radial, m is a mass of H_2O molecule, k is the Boltzmann's constant, u is a velocity of a particle (NH_2 or NH_3) and $\mathrm{erf}(v_{\lambda'})$ denotes the error function. This integral equation can not be solved analytically and inverted generally. However, the approximation which is a two-step predictor-corrector type of solution can be available according to Combi et al.(1993).

Once the particle considered here, NH_3 or NH_2 collides with H_2O molecule (here it is assumed that only H_2O is the target of collisions because H_2O is the most rich component in the nucleus), the velocity of the particle is changed. Combi & Smyth(1988) assumed that the relative velocity of the particle is scattered isotropically in the center of mass system of the particle and H_2O molecule, this assumption is accepted here. The velocity of the target (H_2O molecule) consists of the bulk outflow component and the randomized thermal component (the procedure to determine the velocity is basically same as that for NH_3 molecule).

2.5 Results and Discussions

Although the ammonia molecule is considered as the parent of NH_2 in the previous section, other molecules can be treated as the parent of NH_2 in the collisional random walk model. To calculate the surface brightness profile when other molecule is NH_2 parent, the lifetime and the ejection velocity of the parent molecule should be known. Krasnopolsky & Tkachuk (1991) suggested three possible parents of NH_2, namely NH_3, N_2H_4 and CH_3NH_2, and the lifetimes and ejection velocities are listed for these possible parents. The parameters are also listed in Table 2.2, where only the lifetime of NH_3 is referred from Tegler et al. (1992).

Figure 2.3 shows the surface brightness profile of NH_2 determined by the collisional random walk model for three possible parents of NH_2. The result of Haser's model calculation fitted to the observation is also shown in Figure 2.3. Although Haser's model is not realistic at all, this model gives a good approximation for the observed surface brightness profile (of course there isn't much meaning physically in the scale lengths used for the calculation). The rugged part in the calculation (the nucleocentric distance is less than about $10^{5.5}$ km) is caused by a lack of test particles, a quasi steady-state is still not achieved for this region. The results considering the collisions between molecules indicates that NH_3 is most likely to be parent of NH_2 among three possible parent.

Here, the validity of the used model must be considered. First, in the model the spherically symmetric coma for NH_2 is assumed. Regarding this point, it is generally good approximation to deal with the coma formed by molecular emissions as spherically symmetric. For example, Figure 2.4 shows the C_2 coma of comet C/1996B2 (Hyakutake) was spherically symmetric. Next, it is assumed that the gas production rate was constant in the model. However, it is observed that the water production rate of comet C/1996B2 (Hyakutake) increased day-by-day around 1996 March 23. The influence of increasing water production rate must be considered. The variation of the water production rate per day, $\Delta Q(H_2O)$ molecules s^{-1} day^{-1}, was about 2.4×10^{27} from 1996 March 4 to 1996 March 23 (Watanabe & the SWAT Team 1996). On the other hand, it takes about 3 hours for the molecules to travel from the nucleus to the end of slit at the observation. This variation for 3 hours was less than 1 percent of the water production rate at that time, so it is concluded the model used here were appropriate.

The conclusion is also verified by comparing the ammonia abundance inferred from the observation shown here with the ammonia abundance determined from a radio observation directly. The production rate ratio of ammonia to water, $Q(NH_3)/Q(H_2O)$, is determined to be about 0.5 percent from the observation shown here based on Haser's model (Fink 1994), where it is assumed that $Q(NH_3) = 1.05 \times Q(NH_2)$ according to Magee-Sauer et al. (1989). The production rate of NH_2 is derived from $NH_2(0,8,0)$ emission band and the fluorescence efficiency calculated in Chapter 3 (Table 3.1). The production rate of water is derived from [OI] emission at 6300 Å which is emitted from $O(^1D)$ atom generated from water according to the following reactions:

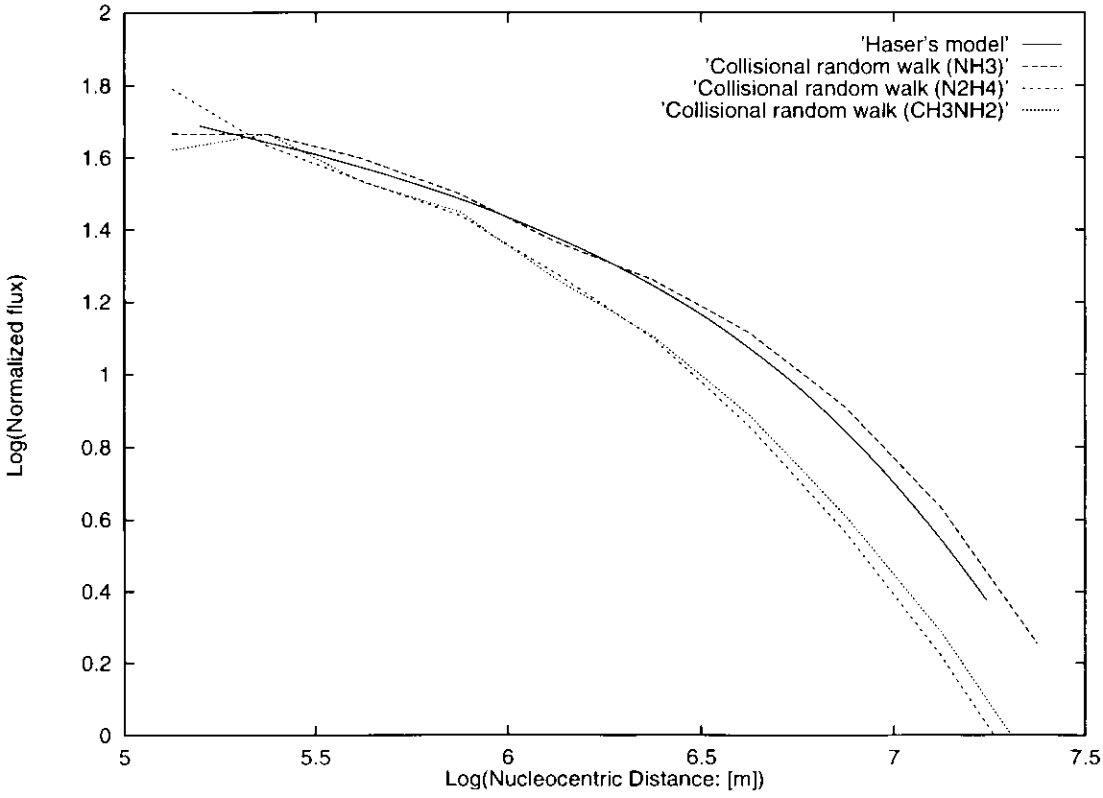

Figure 2.3: The spatial profiles of NH_2 are calculated for three possible candidates (NH_3, N_2H_4 and CH_3NH_2) based on the collisional random walk model. The solid line is best fitted to the observed data using Haser's model. This result indicates that NH_3 is most likely to be parent of NH_2 among three possible parent.

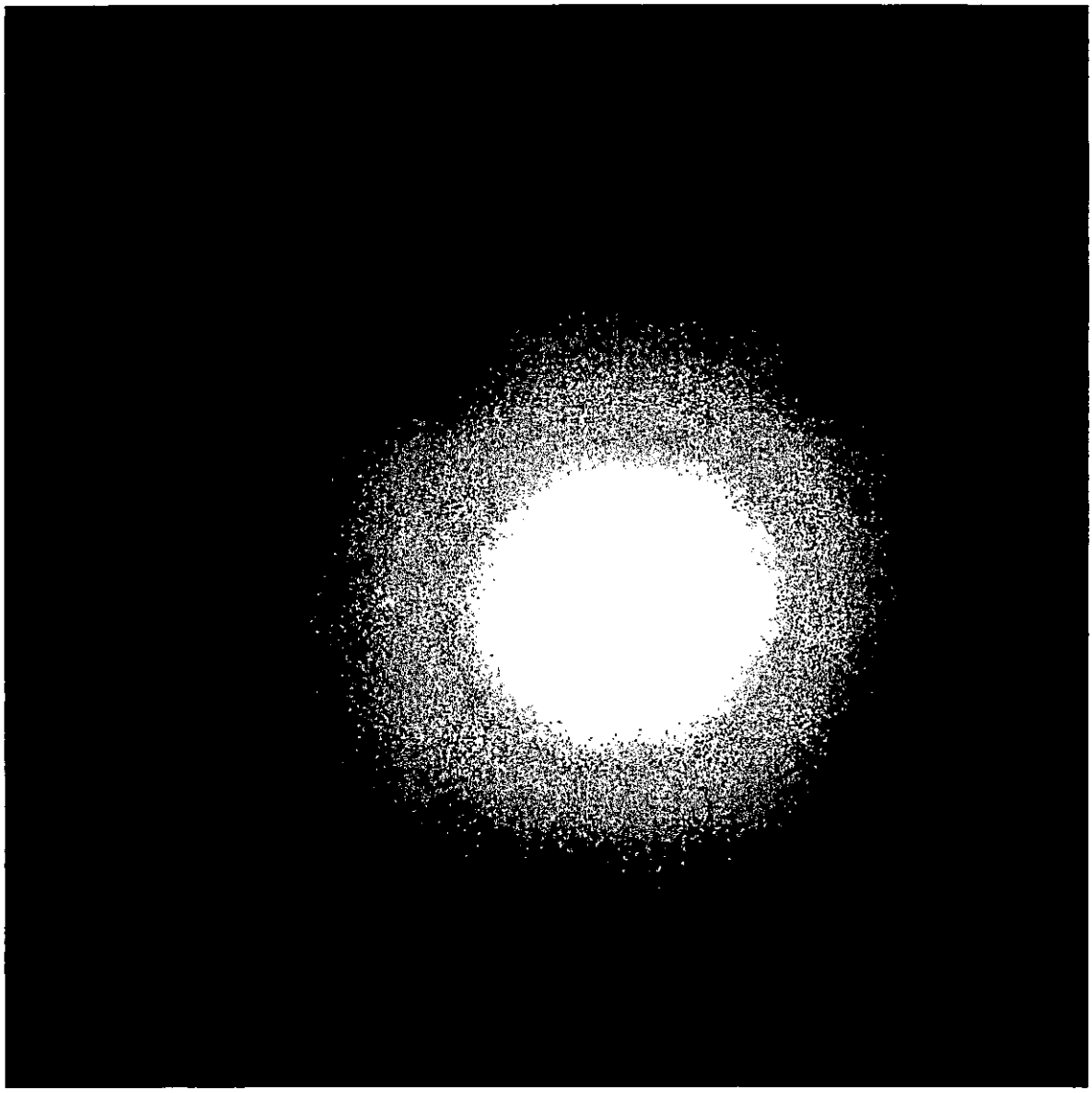

Figure 2.4: C_2 coma of comet C/1996B2 (Hyakutake) observed on April 5 - 6 at National Astronomical Observatory Japan. A narrow-band filter set for C_2 (the emission band and its continuum) was used to determine C_2 coma. This image corresponds to 2.6×10^8 km $\times$ 1.7×10^8 km (Sekiguchi et al. 1996, Sekiguchi 1997).

$$H_2O + h\nu \Rightarrow H_2 + O(^1D), \tag{2.12}$$

$$H_2O + h\nu \Rightarrow OH + H, \tag{2.13}$$

$$OH + h\nu \Rightarrow H + O(^1D). \tag{2.14}$$

On the other hand, Bird et al. (1997b) reported $Q(NH_3)/Q(H_2O)$ was equal to 0.6 percent, which was derived from the radio observation of ammonia on March 23/24(UT). These results are consistent with each other, and also support the conclusion that the NH_2 parent is NH_3.

Festou et al. (1987), however, reported that the NH_2 parent has a fairly short lifetime, of the order of a few hundred seconds at 1 AU (the ammonia molecule doesn't have such a short lifetime) in comet IRAS-Araki-Alcock. Their results were derived from the spectra within the region of 1,500 km in radius surrounding the nucleus. Several reasons are considered about this inconsistency. In Festou et al. (1987) the instrumental transmission function was derived by adjusting the continuum emission due to the cometary dust to a synthetic solar spectrum, so the subtraction of continuum emission within the emission band of NH_2 may be incomplete. Next, because they measured the flux of the NH_2 (0,9,0) band, the short lifetime of NH_2 parent may be caused by the contamination of C_2 ($\Delta v = -2$) band with NH_2(0,9,0) band. This contamination is serious when the C_2 emission is noticeable. For the surface brightness profile of the C_2 emission, they also reported that the one of parents (it is assumed that C_2 radicals have two parents) has a short lifetime, which time scale is close to the lifetime of the NH_2 parent they showed. Therefore, it is thought that the short lifetime of NH_2 parent they reported may be corresponding to the short lifetime of one of parents of C_2 radicals.

2.6 Summary

In this chapter, the parent molecule of NH_2 radicals is discussed via surface brightness profile of NH_2 emission band. Because comet C/1996B2 (Hyakutake) had approached to the Earth very closely and became bright, the surface brightness profile of NH_2 was obtained with small spatial error from a low dispersion spectrum.

The NH_2 (0,8,0) band is selected here in order to avoid the contamination of other strong emission bands such as C_2 Swan band sequences. In the

observation the collisional effects between the molecules should be considered, so these effects are dealt by using the collisional random walk model for NH_2. Three possible parent of NH_2, namely NH_3, N_2H_4 and CH_3NH_2, are considered here for the calculation. Among these candidates, it is found that the ammonia molecules (NH_3) are most likely to be the NH_2 parent by comparing the observed brightness profile with the profile determined from the collisional random walk model for each possible NH_2 parent. This conclusion is also supported from the viewpoint of the production rate of ammonia.

Chapter 3

Fluorescence Excitation Model of NH_2 in Cometary Comae

3.1 Introduction

Emission bands of NH_2 $\tilde{A}(0,v_2',0)$ — $\tilde{X}(0,0,0)$ (hereafter called "$(0,v_2',0)$ band" briefly) are usually recognized in optical cometary spectra when a comet is near 1 AU from the Sun. NH_2 is thought to be a photodissociation product of ammonia as shown in Chapter 2. Therefore, NH_2 is important key to study properties of cometary ammonia. The Ortho-to-para ratio (OPR) is one of primordial characters of a cometary molecule and it has been derived precisely in a few comets for H_2O only (Irvine et al. 2000, Crovisier 1999, Mumma et al. 1987). Although the OPRs of H_2CO and CH_4 were reported as preliminary reports (Womack et al. 1997, Weaver et al. 1997), there is no detailed information or report for them. The OPR of cometary ammonia has never been derived so far.

Direct determination of OPR of ammonia in a comet is difficult because (i) low S/N ratio even for brightest comets (e.g., comet C/1995O1 (Hale-Bopp)) and (ii) difficulties for modeling emission spectrum of ammonia in cometary coma due to collisions between molecules and optically thick condition. In contrast with ammonia, it is easy to obtain high-S/N spectrum of cometary NH_2 in the visible wavelength region, and to model an emission spectrum in cometary coma because NH_2 exists in relatively outer part of coma where it is collision-less and optically thin. The OPR of ammonia can be determined from the OPR of NH_2 derived from high-dispersion spectroscopic observations. The modeling to reproduce the observed rotational structure in NH_2 emission bands is necessary for determining the OPR of NH_2.

The vibrational band structure of NH_2 was calculated by A'Hearn (1982) for the first time. He calculated the fluorescence efficiencies of some bands of NH_2 in optical region. Further study for vibrational structure of $(0,v_2',0)$

bands was performed by Tegler & Wyckoff (1989) based on calculations by Jungen et al. (1980). In the calculation of Tegler & Wyckoff (1989), only vibronic levels were considered (i.e., the rotational structure was neglected). Arpigny (1994) pointed out that the fluorescence efficiencies shown in Tegler and Wyckoff (1989) should be multiplied by 0.5 because only half of NH_2 molecules contributes for each band when the rotational structure is considered. However, Rauer et al. (1997a, 1997b) reported that the flux ratio between even- and odd-v_2' bands was different from that expected from Tegler and Wyckoff (1989) for the comet C/1995 (Hale-Bopp) far from the Sun ($\approx$ 3 AU), and pointed out that the excitation mechanism of NH_2 should be re-examined.

Concerning a rotational structure, the first attempt to reproduce a rotational structure of a NH_2 (0,v_2',0) band was shown in Combi & McCrosky (1991) as a private communication from Wyckoff. The simple fluorescence spectrum of NH_2 (0,8,0) band for rotational temperatures of 20, 60, 200K were shown. These calculations are very simple because it is assumed that only a flat continuum excitation source, rather than a true solar spectrum. More detailed information is unknown for this calculation.

Recently, Glinski et al. (2001) demonstrated that their "photostationary state model" (i.e., a fluorescence equilibrium model) can explain the fine structure of the NH_2 (0,8,0) band for comet C/1995O1 (Hale-Bopp) at 1 AU and 2.6 AU from the Sun. Their model could explain the anomalous band ratio reported by Rauer et al. (1997a) qualitatively. In their model, the transitions between $\tilde{A}$(0,v_2',0) and $\tilde{X}$(0,0,0), as well as the radiative cooling in $\tilde{X}$(0,0,0) state, are considered. However, they calculated the populations of the F_1 levels only, and assumed that the F_2 levels were equilibrated (F_1 and F_2 indicate the sub-levels corresponding to $J = N + 1/2$, $J = N - 1/2$, respectively). Furthermore, the Swings effect (which is caused by the Doppler shift of solar spectrum due to a cometary motion relative to the Sun) was not considered in their model.

In this chapter, in order to determine the OPR of NH_2 precisely, more sophisticated NH_2 model is presented. The model results will be compared with the low-dispersion spectroscopic observation. Comparisons with a high-dispersion spectrum of cometary NH_2 and the OPR of cometary NH_2 will be shown in the next chapter.

3.2 NH_2 Excitation Model in Cometary Coma

The population distribution among energy levels is calculated assuming fluorescence by solar radiation. Both F_1 and F_2 components are included in the model in contrast with Glinski et al. (2001). The NH_2 transitions included in the model are;

(i) the ro-vibronic transitions: $\tilde{A}(0,v_2',0)$—$\tilde{X}(0,v_2'',0)$, $18 \geq v_2' \geq 1$, $v_2'' = 0$ and 1 (Dressler & Ramsay 1959, Johns et al. 1976, Ross et al. 1988, Huet et al. 1996, Hadj Bachir et al. 1999),

(ii) the ro-vibrational transitions of vibrational overtone and hot bands: $\tilde{X}(0,v_2',0)$—$\tilde{X}(0,v_2'',0)$, $13 \geq v_2' \geq 8$, $v_2'' = 0$ and 1 (Ross et al. 1988, Huet et al. 1996, Hadj Bachir et al. 1999),

(iii) the ro-vibrational transitions of vibrational fundamental bands: $\tilde{X}(1,0,0)$—$\tilde{X}(0,0,0)$ (ν_1), $\tilde{X}(0,1,0)$—$\tilde{X}(0,0,0)$ (ν_2), and $\tilde{X}(0,0,1)$—$\tilde{X}(0,0,0)$ (ν_3) (Burkholder et al. 1988, McKellar et al. 1990), and

(iv) the pure rotational transitions in $\tilde{X}(0,0,0)$ (Ross et al. 1988) .

The transitions of $\tilde{A}(0,v_2',0)$—$\tilde{X}(0,v_2",0)$ occur according to the c-type selection rule (ΔK_a=1,3 and ΔK_c=0,2 are considered). The other transitions except $\tilde{X}(0,0,1)$—$\tilde{X}(0,0,0)$ occur according to the b-type selection rule (ΔK_a=1,3 and ΔK_c=1,3 are considered) while $\tilde{X}(0,0,1)$—$\tilde{X}(0,0,0)$ occur according to the a-type selection rule (ΔK_a=0,2 and ΔK_c=1,3 are considered) (Townes & Schawlow 1975).

The Einstein "A" coefficient related to a transition between an upper level "2" and a lower level "1", A_{21}, can be given as

$$A_{21} = \frac{64\pi^4\nu_{21}^3}{3hc^3}|\mu_{21}|^2, \tag{3.1}$$

where h denotes Planck's constant, c the speed of light, ν_{21} a frequency of the emission, and μ_{21} a matrix element of the transition moment (Herzberg 1950).

The preceding formula apply to the case of transitions between non-degenerate levels only. In the case of a transition between two degenerate levels of degeneracy d_2 and d_1, the above formula should be replaced by

$$A_{21} = \frac{64\pi^4 \nu_{21}^3}{3hc^3} \frac{\sum |\mu_{21}|^2}{d_2}, \tag{3.2}$$

where the summation should be done for all sublevels (Herzberg 1950).

The Einstein "B" coefficients between upper and lower levels are given as

$$B_{21} = \frac{c^3}{8\pi h \nu_{21}^3} A_{21}, \tag{3.3}$$

$$B_{12} = \frac{d_2}{d_1} B_{21}. \tag{3.4}$$

The number of upward transition by solar radiation per cm^3 per second is given as $N_1 B_{12} \rho(\nu_{12})$ where N_1 is the number of molecules per cm^3 in the lower level "1" and $\rho(\nu_{12})$ is a solar radiation density at frequency of ν_{12}. The $\rho(\nu_{12})$ is expressed in terms of energy per cm^3 per unit frequency interval.

A high-dispersion solar spectrum is necessary for calculating the solar radiation density. The solar spectrum obtained by Kurucz et al. (1984) and the spectrum calculated based on Kurucz (1992) are used for optical and near-infrared region (from 296nm to 200μm). The solar spectrum in infrared region (from 200μm to 1mm) is also used (Thekaekara 1974). The Doppler shift caused by the cometary motion is considered in calculating the solar radiation density. Any variations with solar activity are not considered here. These effects should be less than 1 % because the solar flux pumping the fluorescence is confined to wavelengths for which the solar flux is almost insensitive to solar activity (A'Hearn et al. 1995).

The μ_{21} can be easily calculated for a diatomic or a linear poly-atomic molecule, e.g., HCN, CO_2, CO, C_2, CN (Rohlfs & Wilson 1996). However, NH_2 molecule is a bent, asymmetric top molecule. Therefore, the matrix elements of the transition moment are calculated in the following manner.

Case (i): Electronic Transitions

The matrix element of transition moment can be expressed as the product between the vibronic ("vibrational and electronic") part and the rotational part. The vibronic part is taken from the table 7 in Jungen et al. (1980). The Σ, Π, Δ, Φ, and Γ sub-bands are listed in the table. These sub-bands

are included in the model. Using the value listed in the table, the electronic transition moment of $\tilde{A}$–$\tilde{X}$ system must be multiplied (Jungen et al. 1980).

The rotational part is calculated using ASYROT program code (Birss & Ramsay 1984). The relative intensities of rotational lines can be calculated by the ASYROT program under assumption that all rotational lines belong to the same vibronic transition. The relative intensity is calculated by

$$I_{\mathrm{ASYROT}} = g_I \ \exp\left(-E_i/kT\right) \ S_{rot}, \tag{3.5}$$

where g_I is a nuclear spin statistical weight, $\exp\left(-E_i/kT\right)$ is a Boltzmann factor, and S_{rot} is a rotational line strength.

The molecular constants of the upper electronic state $\tilde{A}(0,v_2',0)$, the ground state $\tilde{X}(0,0,0)$, and $\tilde{X}(0,1,0)$ used in the ASYROT calculation are given in Dressler & Ramsay (1959), Johns et al. (1976), Ross et al. (1988), Burkholder et al. (1988), Huet et al. (1996), and Müller et al. (1999). The correctness of the ASYROT calculation is confirmed in the case of H_2O^+ (Lew 1976) as well as that of pure rotational transitions (Townes & Schawlow 1975). Please note that the calculation by ASYROT does not take into account the electron spin structure. Regarding the line splitting caused by unpaired electron ($S = 1/2$) of NH_2 (the hyperfine splitting caused by the nitrogen atom could not be resolved in the spectra shown in this thesis), the relative intensities between the spin doublet lines are calculated by a conventional expression (Sears 1984). Here, the table of Appendix I in Townes & Schawlow (1975) was used for calculating relative intensities of the spin doublet lines (in order to use this table, I, J, and F should be replaced by S, N, and J, respectively).

Finally, the square of matrix element of transition moment is obtained as

$$|\mu_{2\,1}|^2 = |\mu_{2\,1}^{vibronic}|^2 S_{rot}, \tag{3.6}$$

where $\mu_{2\,1}^{vibronic}$ is a vibronic transition moment determined above according to Jungen et al. (1980) and S_{rot} should be corrected for the electron spin structure as described above.

Case (ii): Overtone Vibrational Transitions

The calculation of transition moment for $\tilde{X}(0,v_2',0)$—$\tilde{X}(0,v_2'',0)$ where $13 \geq v_2' \geq 8$, $v_2'' = 0$ and 1, is basically same for the case (i) described above.

The matrix element of transition moment can be expressed as the product between the vibrational part and the rotational part. The vibrational part is taken from the table 7 in Jungen et al. (1980) where these values were normalized by the electric dipole moment. Therefore, the value listed in the table should be multiplied by the electric dipole moment in $\tilde{X}$ state (Buenker et al. 1981). The rotational part can be determined by ASYROT program. The molecular constants for ASYROT are given in Dressler & Ramsay (1959), Johns et al. (1976), Ross et al. (1988), Burkholder et al. (1988), Huet et al. (1996), and Müller et al. (1999).

Case (iii): Fundamental Vibrational Transitions

For the vibrational fundamental bands of NH_2, the matrix element of transition moment is divided into the vibrational part and the rotational part. The vibrational transition moment is determined by *ab initio* calculations using MOLPRO2000 and SURVIBTM program (Ermler et al. 1988) for the ν_1 and ν_2 fundamental bands. The vibrational transition moment of the ν_3 fundamental band is determined under the assumption that the ratio of vibrational transition moments between ν_1 and ν_3 is equal to about 4 (Amano et al. 1982). The rotational part can be determined by ASYROT program. The molecular constants for ASYROT are given in Burkholder et al. (1988), McKellar et al. (1990), and Müller et al. (1999).

Case (iv): Rotational Transitions

The rotational transition moment μ_{21}^{rot} is determined from the equation,

$$S_{rot} = (2J+1)\frac{|\mu_{21}^{rot}|^2}{\mu^2} \tag{3.7}$$

where J is a quantum number of total angular momentum and μ is a relevant electric dipole moment (Townes & Schawlow 1975).

The permanent dipole moment μ is determined from *ab initio* calculations using GAUSSIAN98, 1.81 Debye. This value is consistent with the experimental value of 1.82±0.05 Debye for NHD (Brown et al. 1979). The S_{rot} is calculated by ASYROT program using molecular constants of $\tilde{X}$(0,0,0) (Müller et al. 1999).

The rotational levels with $N \leq 4$ are included, since Tegler & Wyckoff

(1989) mentioned that the NH_2 rovibronic lines for $N > 4$ were usually not recognized in the cometary spectra. Thus, the 818 levels and 8473 transitions are included in the model calculation here.

The excitation mechanism for observed NH_2 emission bands in optical cometary spectra is dominated by resonance fluorescence as Tegler & Wyckoff (1989) demonstrated. They showed that the fluorescence excitation rate for each NH_2 molecule in a ground state to upper vibronic state is $\approx 4 \times 10^{-3}$ s^{-1} for a typical NH_2 ($\tilde{A}$–$\tilde{X}$) band at 1 AU from the Sun. This value corresponds to ≈ 3 minutes. On the other hand, NH_2 molecules excited into vibronic state are produced through the photodissociation of ammonia as follows (Biesner et al. 1989, Tegler & Wyckoff 1989);

$$NH_3 + h\nu(\lambda \leq 2060\mathring{A}) \rightarrow NH_2(\tilde{A}^2A_1) + H. \tag{3.8}$$

The photodissociation rate of ammonia at 1 AU from the Sun is estimated as 1.70 — 1.87×10^{-4} s^{-1} (Huebner et al. 1992) and the branching ratio or fractional yield into $NH_2(\tilde{A}^2A_1)$ state is about 0.1 (Suto & Lee 1983). Thus the rate of prompt emission from $NH_2(\tilde{A}^2A_1)$ produced from above reaction is about 1.8×10^{-5} s^{-1}, corresponding to ≈ 14 hr (Tegler & Wyckoff 1989). It is clearly shown that fluorescence dominates prompt emission as an excitation mechanism in a comet.

The typical life time of upper $\tilde{A}$ state of NH_2 is ≈ 10 μs and is negligible in comparison with the time scale of absorption of solar photon, 175 s at 1 AU. Thus almost cometary NH_2 are in their electronic ground state (Tegler & Wyckoff 1989). Since the photodissociation rate of NH_2 is 2.15 — 3.40×10^{-6} s^{-1} (Huebner et al. 1992) and the ratio of the fluorescence rate relative to the photodissociation rate of NH_2 is ≈ 1000, namely about 1000 upward transitions occur for each NH_2 molecule before its dissociation. A fluorescence equilibrium for NH_2 molecules can be assumed in a cometary coma.

The population distribution of NH_2 is determined by solving fluorescence equilibrium equations assuming an optically thin condition in cometary coma (A'Hearn 1978). The fluorescence equilibrium equations are the same as the equation (1) in A'Hearn (1978),

$$x_i[\sum_{j\neq i}(A_{ij} + B_{ij}\rho(\nu_{ij}))] = \sum_{j\neq i}[x_j(A_{ji} + B_{ji}\rho(\nu_{ji}))], \tag{3.9}$$

where x_i is a population of level "i", A_{ij} and B_{ij} are Einstein coefficients for the transition from "i" to "j", and $\rho(\nu_{ij})$ is a solar radiation density at

frequency of ν_{ij} corresponding to the transition.

For the NH_2 case, two sets of equations are obtained according to the equation (3.9). One set is for ortho-NH_2 and the other is for para-NH_2. In each set of equations one equation is redundant and it must be replaced with a normalization equation for the fractional populations,

$$\sum_i x_i = 1. \tag{3.10}$$

The equations are solved numerically by the singular value decomposition method (Press et al. 1992). The abundance ratio of ortho-NH_2 to para-NH_2 is a free parameter for synthesizing NH_2 emission spectrum.

3.3 Model Results and Discussions

Figure 3.1 shows the comparison between an observed cometary spectrum and a modeled spectrum of NH_2. The cometary spectrum is of comet C/2001A2 (LINEAR) taken by 65cm telescope and a low dispersion spectrograph ($\lambda/\Delta\lambda$=500) on 2001 July 12 (UT). The heliocentric and geocentric distance of the comet were 1.2 AU and 0.3 AU at the observation, respectively. The slit was put on the optical center of coma. The C_2 emission (Swan) bands and the forbidden emission lines of atomic oxygen as well as NH_2 emission bands are shown in the observed spectrum. The modeled spectrum of NH_2 emission bands can reproduce the observation well for this case.

The fluorescence efficiencies of NH_2 are calculated and listed in Table 3.1. The heliocentric radial velocity is assumed to be 0 km s^{-1} and the ortho-to-para ratio of NH_2 is assumed to be 3 in this calculation (the ratio of statistical weights between ortho- and para-NH_2 is 3). Please note that the model results are multiplied by $(A_{v_2' \, 0} + A_{v_2' \, 1})/\Sigma_{\text{for all } v_2''}(A_{v_2' v_2''})$ calculated from the table 7 in Jungen et al.(1980) because the transitions of $\tilde{A}(0,v_2',0)$—$\tilde{X}(0,v_2'',0)$, $v_2'' \geq 2$, are not considered in the model calculation. The values in the table have been already corrected.

In Chapter 2, it is shown that the ammonia abundance, $Q(NH_3)/Q(H_2O)$, determined from NH_2 using the value in Table 3.1 is consistent with that determined directly from the radio observation of ammonia in the case of C/1996B2 (Hyakutake). This fact supports the validity of the model calculations.

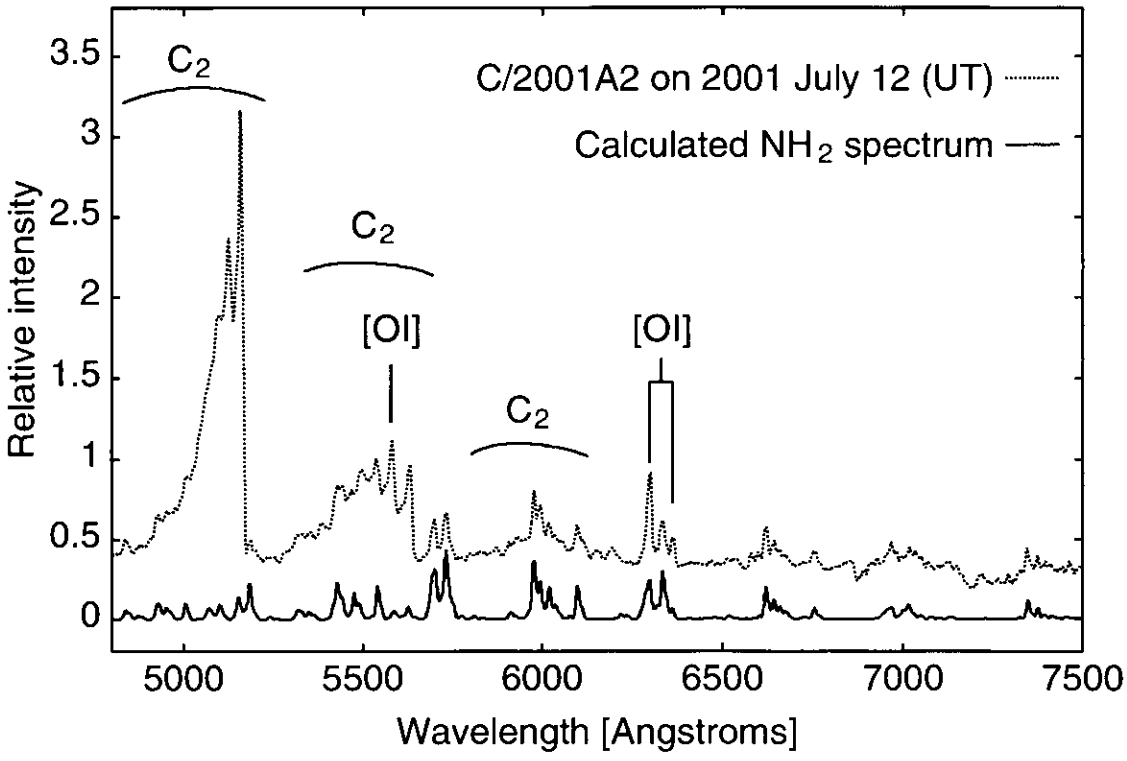

Figure 3.1: The comparison between a low dispersion cometary spectrum and a modeled NH_2 spectrum. The cometary spectrum is of comet C/2001A2 (LINEAR) on 2001 July 12 (UT) taken by 65cm telescope and a low dispersion spectrograph ($\lambda/\Delta\lambda$=500). The modeled spectrum is calculated for the comet and the spectral resolution is adjusted to be the same as the observed spectrum. The emission bands of C_2 and forbidden emission lines of atomic oxygen as well as NH_2 emission bands are recognized in observed spectrum.

The validity of the revised NH_2 fluorescence efficiencies can be also confirmed by comparing ammonia abundance determined from NH_2 and that from *in situ* observation in the case of comet 1P/Halley. Ammonia abundance in comet 1P/Halley can be re-determined from the observation of Wyckoff et al. (1991), and it should be compared with that estimated from Giotto mass spectrometer measurements (Meier et al. 1994), $1.5^{+0.5}_{-0.7}$ %. The revised NH_2 fluorescence efficiency leads to the ammonia abundance of 0.75±0.18 %, which is consistent with *in situ* measurements. The ammonia abundance estimated from UV spectra of NH radical was 0.44 — 0.94 % (Feldman et al. 1993), which is also consistent with above values.

Figure 3.2 shows the variation of fluorescence efficiencies with respect to a heliocentric distance. The dependency on a heliocentric distance is different between even- and odd-v_2' bands. Furthermore, these dependencies are different from R_h^{-2} (hereafter, R_h denotes a heliocentric distance) as assumed in Tegler & Wyckoff (1989) and the other studies.

Figure 3.3 shows the variation of a ratio between fluorescence efficiencies with respect to heliocentric distances. Glinski et al. (2001) demonstrated that a larger ratio of the population in even-Ka'' (related to even-v_2' bands) exists relative to that in odd-Ka'' (related to odd-v_2' bands) for a larger heliocentric distance because of the low rotational temperature in the ground state $\tilde{X}(0,0,0)$, and they pointed out that this behavior was consistent with the flux ratio anomaly between the even- and odd-v_2' bands in comet C/1995O1 (Hale-Bopp) at $\approx$ 3 AU from the Sun (Rauer et al. 1997a). Such behavior is also shown in the present model results. The ratio of the fluorescence efficiencies between the even- and odd-v_2' bands depends on the heliocentric distance as shown in Figure 3.3. Note that the ratio given by Tegler and Wyckoff (1989) is constant with respect to the heliocentric distance. That is, for a larger heliocentric distance, the ratio of the even-v_2' band relative to the odd-v_2' band becomes larger, which is consistent with the observation of Rauer et al. (1997a).

Figure 3.4 – 3.7 show the model results assuming OPR of NH_2 to be 3, a heliocentric distance of 1 AU, a heliocentric radial velocity of 0 km s^{-1}. A spectral resolution ($\lambda/\Delta\lambda$) is assumed to be 30000. Figure 3.4 – 3.7 correspond to NH_2 (0,10,0), (0,9,0), (0,8,0), and (0,7,0) band, respectively. These bands are strong and thought to be easy to extract from a cometary spectrum because there are no significant contaminations by other strong emission bands (e.g., C_2 Swan band). For (0,8,0) band, it is difficult to discriminate only para-NH_2 lines because ortho- and para-lines mixed each

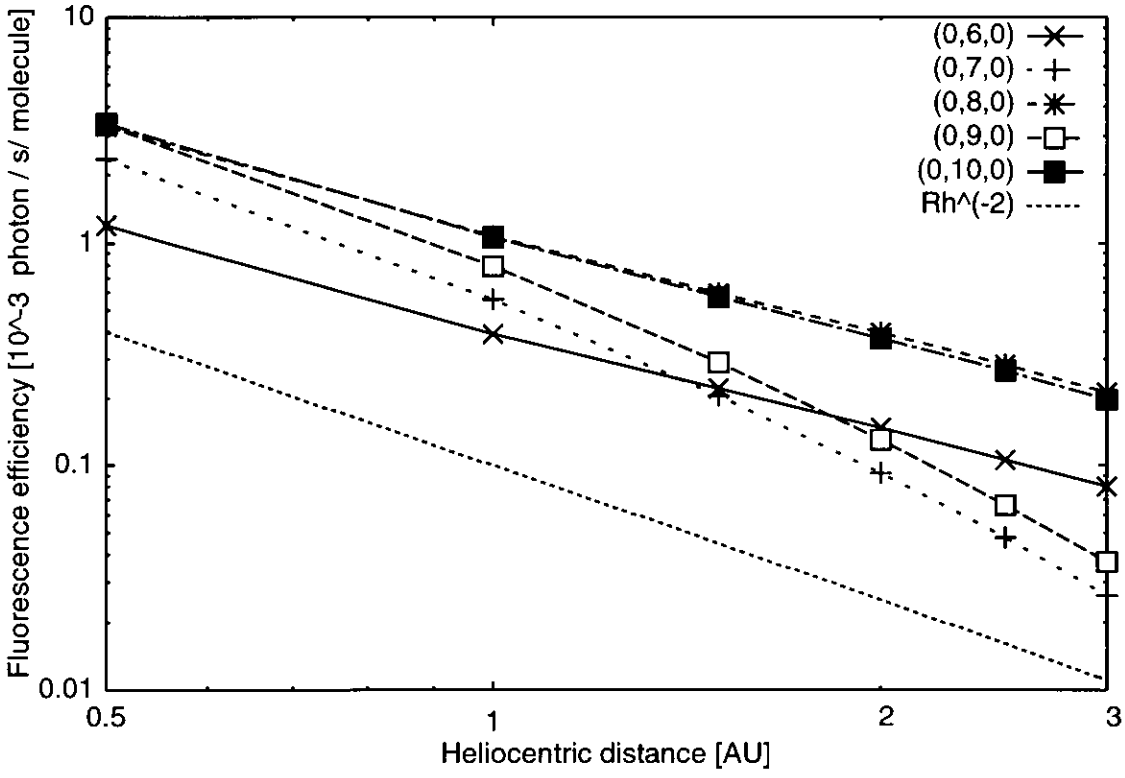

Figure 3.2: The variation of NH_2 fluorescence efficiencies for several bands (from Table 3.1). Note that the dependency with respect to a heliocentric distance is different between even- and odd-v_2' bands. These dependency is different from R_h^{-2} as assumed by Tegler & Wyckoff (1989).

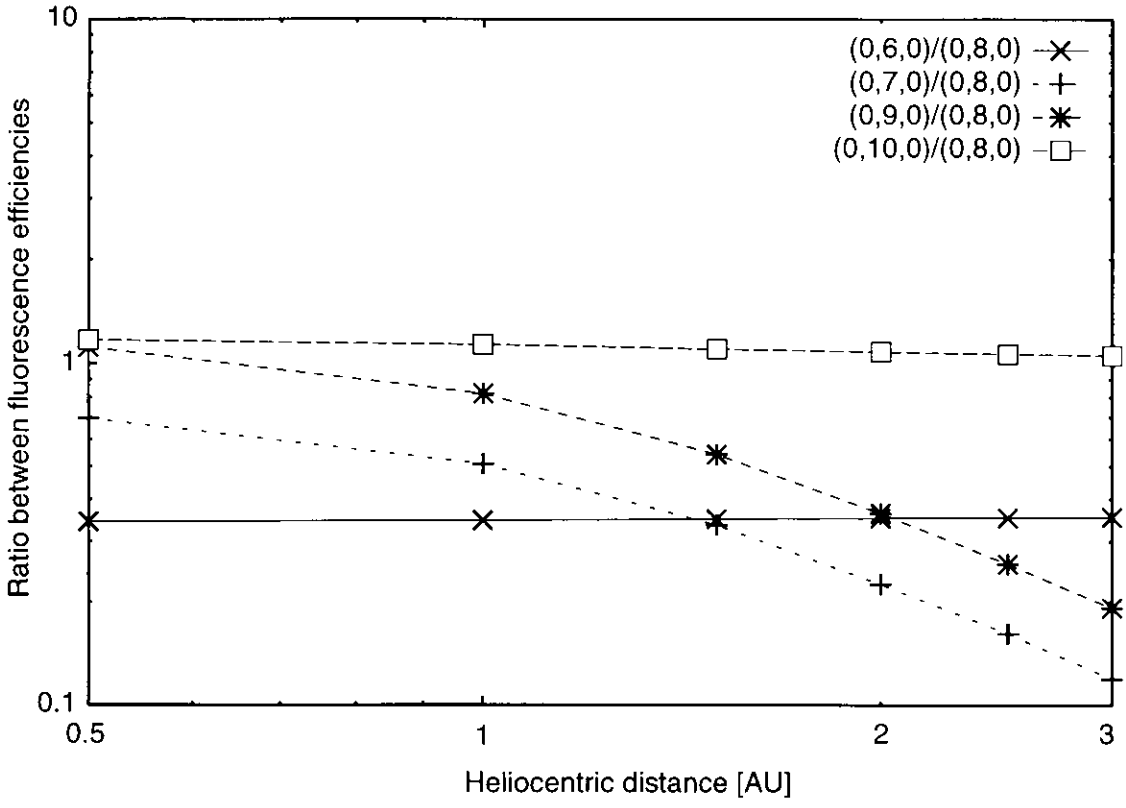

Figure 3.3: The variation of the ratio of NH_2 fluorescence efficiencies. Note that the ratio between even- and odd-v_2' bands depends on a heliocentric distance while the ratio between even-v_2' bands or between odd-v_2' bands is near constant.

Table 3.1: NH_2 fluorescence efficiencies for various heliocentric distances.[a]

NH_2 band	0.5 AU	1 AU	1.5 AU	2 AU	2.5 AU	3 AU	R_h AU[b]
$\tilde{A}$(0,6,0)Π	1.20	0.390	0.220	0.147	0.106	8.00×10^{-2}	0.92 R_h^{-2}
$\tilde{A}$(0,7,0)Σ	2.37	0.561	0.206	9.24×10^{-2}	4.73×10^{-2}	2.63×10^{-2}	2.04 R_h^{-2}
$\tilde{A}$(0,8,0)Π	3.30	1.07	0.594	0.394	0.283	0.213	2.48 R_h^{-2}
$\tilde{A}$(0,9,0)Σ	3.33	0.790	0.290	0.130	6.63×10^{-2}	3.69×10^{-2}	3.00 R_h^{-2}
$\tilde{A}$(0,10,0)Π	3.39	1.06	0.575	0.373	0.266	0.199	2.65 R_h^{-2}

[a] Units: $\times10^{-3}$ photons s^{-1} $molecule^{-1}$. It is assumed that the heliocentric velocity is 0 km s^{-1} and the ortho-to-para ratio of NH_2 is 3 (see text). [b] Tegler & Wyckoff (1989), Arpigny (1994).

other in the assumed spectral resolution. In order to fit the model results with observed spectra to determine OPR of NH_2, the NH_2 bands where the strong ortho- and para- lines exist apart from each other are better. For (0,10,0) band, it is also difficult to extract only para-NH_2 lines, and it is known that there are perturbations for levels related to (0,10,0) band (Ross et al. 1988). Thus, (0,8,0) and (0,10,0) bands are not suitable for a determination of OPR value, at least for the spectral resolution of 30000. NH_2 (0,9,0) and (0,7,0) bands are suitable for fitting between model result and observations to determine an OPR value.

3.4 Summary

In this chapter, sophisticated NH_2 excitation model is introduced. The model includes the electronic, vibrational, rotational, and electron spin structure of NH_2 (818 levels and 8473 transitions were considered). The Swings effect is also considered. The NH_2 emission lines for various heliocentric distances can be determined based on the excitation model assuming the fluorescence equilibrium.

The present model can reproduce the low dispersion NH_2 spectrum at near 1 AU from the Sun. The flux ratio between different NH_2 $\tilde{A}$ – $\tilde{X}$ bands can be calculated. The NH_2 band flux anomaly observed in comet C/1995O1 (Hale-Bopp) by Rauer et al. (1997a) can be explained well by the model described here.

The fluorescence efficiencies of NH_2 are revised based on the present model, and they are useful for the determination of ammonia abundance in comets. The ammonia abundance determined from NH_2 using the revised fluorescence efficiency is consistent with that determined by radio

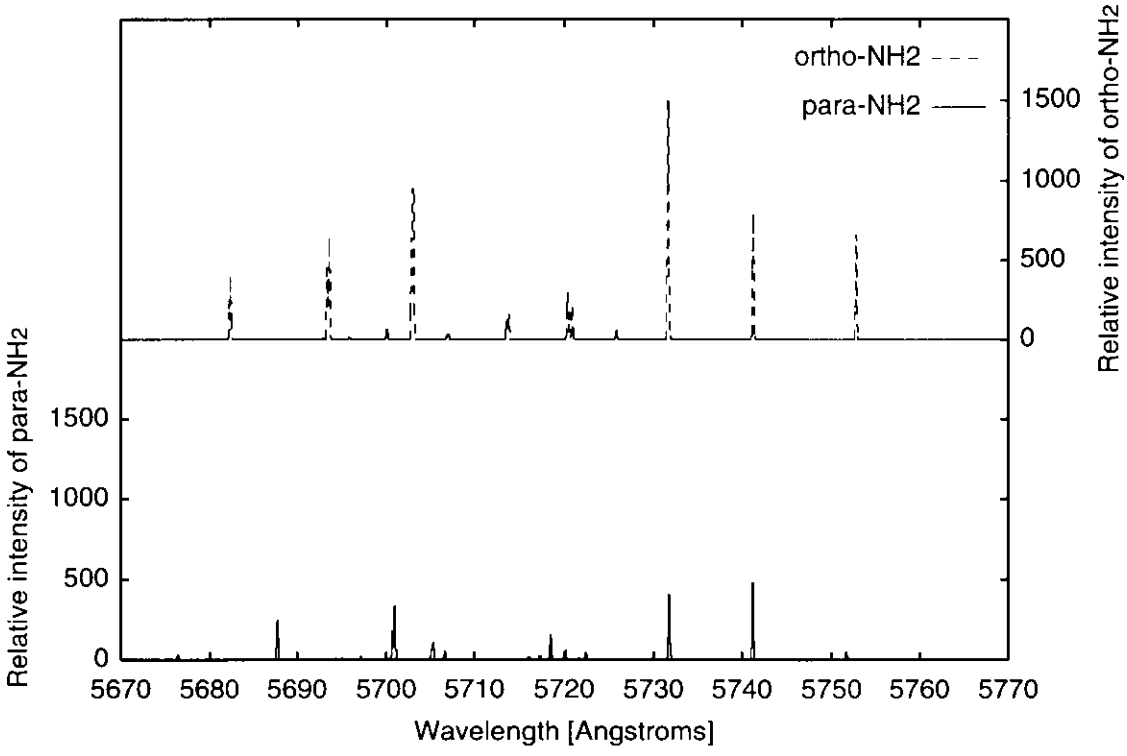

Figure 3.4: Calculated spectrum of NH_2 (0,10,0) band based on the fluorescence model assuming OPR of 3, a heliocentric distance of 1 AU, and a heliocentric radial velocity of 0 km s^{-1}. A spectral resolution ($\lambda/\Delta\lambda$) is 30000.

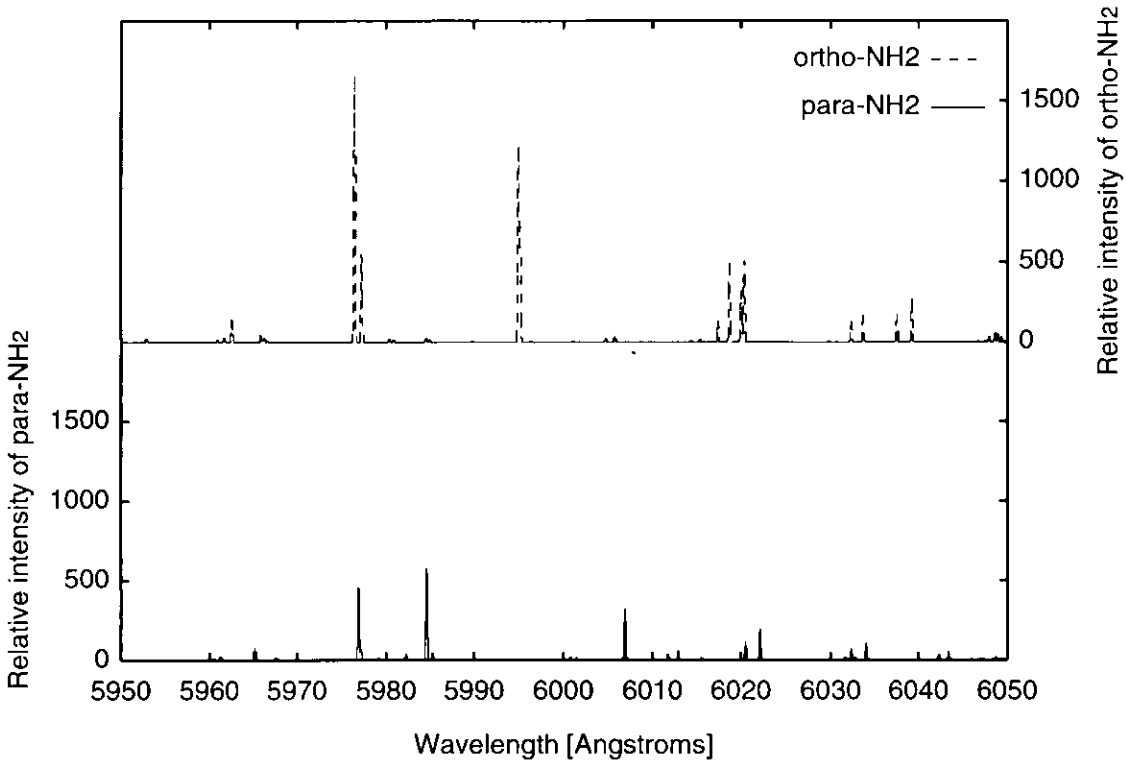

Figure 3.5: Calculated spectrum of NH_2 (0,9,0) band based on the fluorescence model (the conditions are the same as for Figure 3.4).

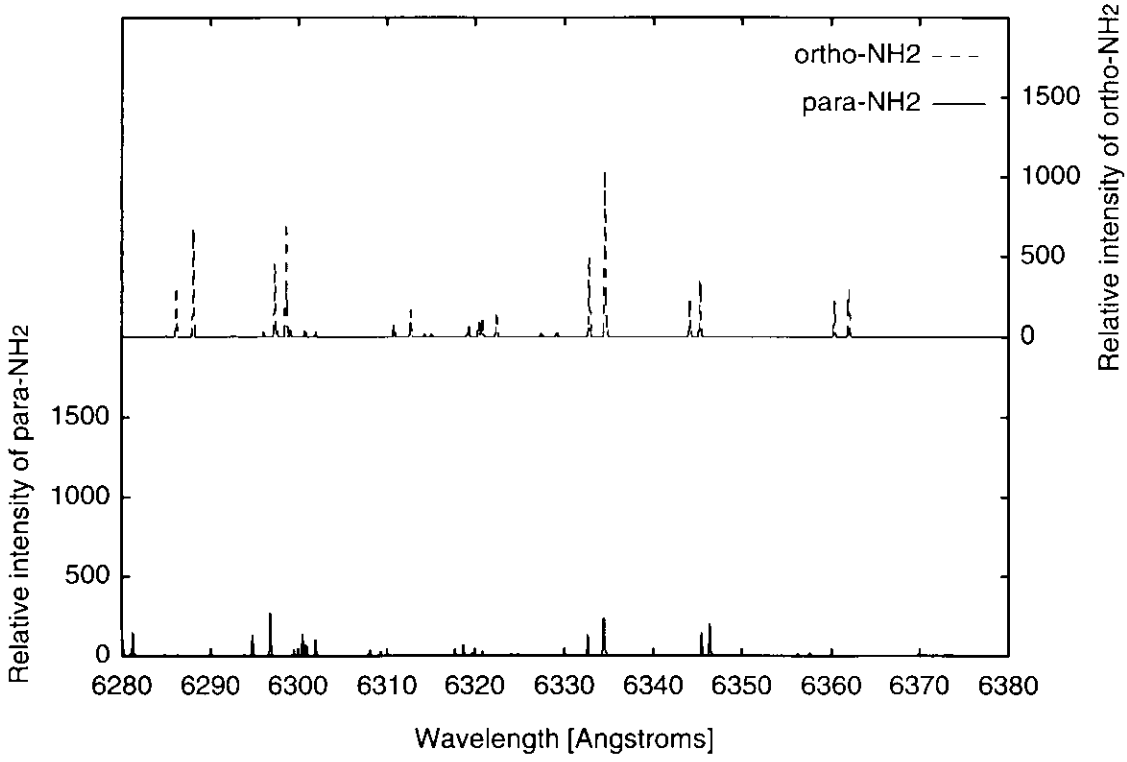

Figure 3.6: Calculated spectrum of NH_2 (0,8,0) band based on the fluorescence model (the conditions are the same as for Figure 3.4).

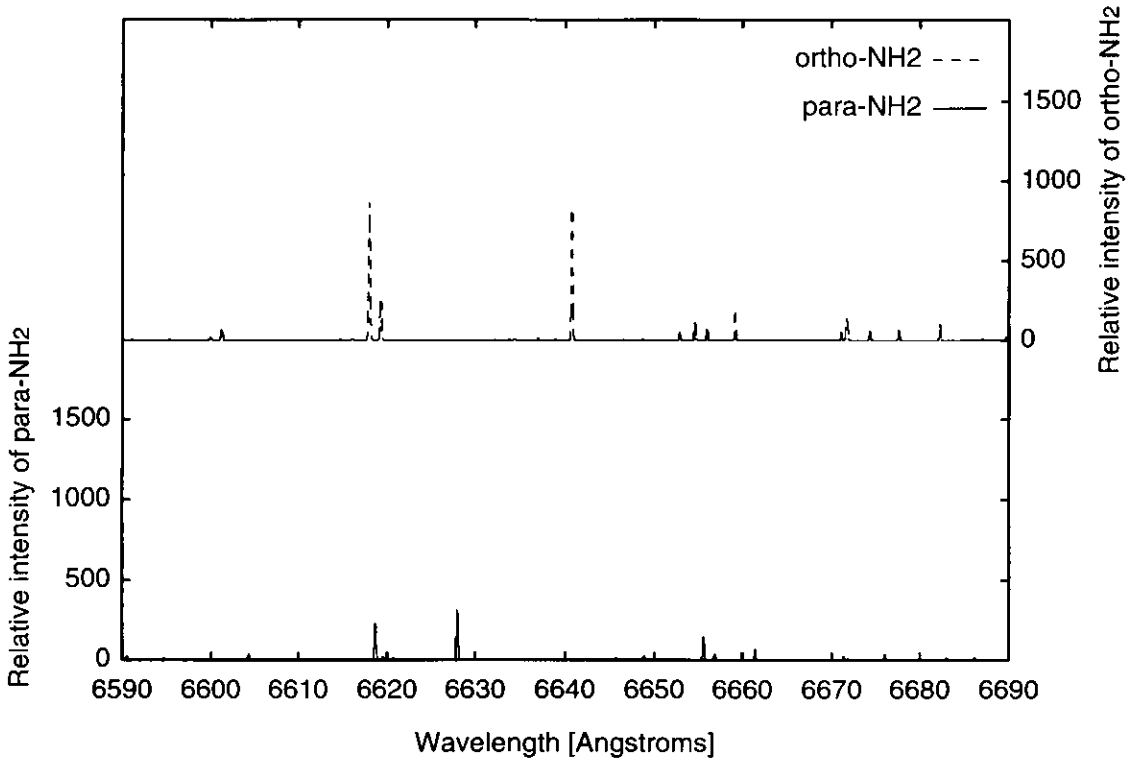

Figure 3.7: Calculated spectrum of NH_2 (0,7,0) band based on the fluorescence model (the conditions are the same as for Figure 3.4).

observations of ammonia directly in the case of C/1996B2 (Hyakutake) as shown in Chapter 2. The validity of revised fluorescence efficiencies is also confirmed in the case of 1P/Halley by comparing ammonia abundance among that determined from NH_2, NH, and *in situ* measurements of NH_3 by Giotto spacecraft.

Thus, it is ready to determine OPR of NH_2 from an actual or observed high-dispersion cometary spectrum based on the NH_2 excitation model. From a viewpoint of contaminations by other strong molecular bands and a separation between ortho- and para-lines, NH_2 (0,9,0) and (0,7,0) bands are suitable for fitting calculated NH_2 spectra to observed spectra in order to determine its OPR value.

Chapter 4

Ortho to Para Ratio of Cometary Ammonia

4.1 Introduction

Comets are thought to be precious relics preserving information on the early solar nebula. In order to investigate the physical conditions of the solar nebula, one important line of inquiry is to study the chemical composition of comets. Recent progress in modeling chemical evolution of the solar nebula allows us to compare the model results with the observed chemical composition of comets (Aikawa et al. 1999, Bockelée-Morvan et al. 2000). A second line of inquiry involves the isotopic composition of comets, especially the deuterium-to-hydrogen (D/H) ratio of water (H_2O) and hydrogen cyanide (HCN) that have been investigated in the recent studies (Mousis et al. 2000, Aikawa & Herbst 1999, Blake et al. 1999, Meier et al. 1998a, 1998b).

Another important key to understanding conditions of the early solar system is the ortho-to-para ratio (OPR). The spin temperature determined from the OPR is believed to be primordial because the spin conversions between the ortho and para species through non-destructive collisions and radiative transitions are strictly forbidden (Irvine et al. 2000).

The first determination of the OPR of a cometary molecule was performed for water in comet 1P/Halley (Mumma et al. 1987) and has been subsequently determined in only three other comets; C/1986P1 (Wilson), C/1995O1 (Hale-Bopp), and 103P/Hartley 2 (Crovisier 1999, Mumma et al. 1993). The observations must be performed from an airplane or a satellite (e.g., Kuiper Airborne Observatory, or Infrared Space Observatory) to avoid the influence of telluric water vapor. Three of these comets (1P/Halley, C/1995O1 (Hale-Bopp), and 103P/Hartley 2) showed that the spin temperature of water was about 25 — 35 K. However, comet C/1986P1 (Wilson) showed the spin temperature higher than 50 K. Irvine

et al. (2000) pointed out that the determination for comets 1P/Halley and C/1986 (Wilson) was hampered by the difficulty in modeling opacity effects and because only part of the ν_3 vibrational band of water was observed. In contrast, the full band of water ν_3 vibrational transitions was observed and the opacity was found to be moderate in ISO observations for C/1995O1 (Hale-Bopp) and 103P/Hartley 2. It is thought that the spin temperature of about 30 K for the comets may reflect the formation temperature of cometary water (Mumma et al. 1993). This temperature range is consistent with that determined from D/H ratios in comets.

In comet C/1996B2 (Hyakutake), Biver et al. (1999) reported OPR of formaldehyde (H_2CO), 1.7±0.3 (corresponding to the spin temperature of 11 K), from radio observations. Derived spin temperature of H_2CO is much lower than the spin temperatures of water ever determined. However, they noted that readers must be very careful for their result because the calibration uncertainties were large due to low atmospheric transmission for para-H_2CO lines. Furthermore, the collision cross sections for the transitions of H_2CO are poorly known. This situation makes it difficult to calculate emission strengths of rotational transitions. There is also a preliminary report on OPR of H_2CO in comet C/1995O1 (Hale-Bopp) by Womack et al. (1997). However their result depends strongly on the population in unobserved levels. More sophisticated investigation is required for this case. A preliminary report on the ratio between nuclear spin species of methane (CH_4) in comet C/1996B2 (Hyakutake) existed (Weaver et al. 1997), and the spin temperature $\geq$ 50 K was shown, but there is no detailed information. Thus, no reliable spin temperature of cometary material has been estimated except water so far. In this chapter, the first determination of the OPR of NH_2, which is thought to be produced from ammonia, is reported.

Ammonia (NH_3) is important in comets as a reservoir of nitrogen atoms and is a key product in the network of chemical reactions related to the nitrogen atoms in the solar nebula (Aikawa et al. 1999). The OPR of cometary ammonia is important for investigations on the chemical evolution and physical conditions in the early solar system. However, the OPR of cometary ammonia has never been determined although ammonia has been detected for a few comets (Bird et al. 1997a, 1997b). Because ammonia exists only near the nucleus where collisions between molecules are dominant, the collisional excitation and de-excitation of the ammonia molecule must be considered to calculate its emission spectrum in the coma.

Although collisions between ammonia and water is especially important in the coma, the precise collision cross section is not known. Furthermore, optically thick conditions near the nucleus requires detailed radiative transfer calculations in the coma to determine the OPR of ammonia.

These conditions make it difficult to calculate accurately the strength of emission from the ammonia molecules in the coma as pointed out by Mumma et al. (1993). Moreover, it is difficult to obtain the ammonia spectra with a high S/N ratio using the existing facilities. Even for the brightest comet in the past decade, C/1995O1 (Hale-Bopp), the obtained spectra of ammonia (e.g., Bird et al. 1997a) did not have sufficient S/N ratio to determine an accurate OPR. The OPR of ammonia can be determined from the data of Bird et al. (1997a) assuming Boltzmann distribution among energy levels of ammonia. In their data there were four measurements of para lines and one measurement of ortho line in comet Hale-Bopp. The excitation temperature of para-ammonia could be determined from these data. Assuming the excitation temperature of ortho-ammonia is equal to that of para-ammonia, the OPR of ammonia could be derived as 0.6 — 1.8 for comet Hale-Bopp. This result can give just lower limit of spin temperature only ($\geq$ 17 K). It should be note that the measurement of OPR is difficult because it usually involves assumptions about the population of unobserved levels and often involves the calibration uncertainties associated with observing at different frequencies and different times as pointed out by Irvin (1999).

On the other hand, most of the NH_2 molecules in comets are thought to be photodissociation products of ammonia as shown in Chapter 2 (Kawakita & Watanabe 1998, Tegler et al. 1992, Fink et al. 1991). Although NH_2CHO which is an other possible parent of NH_2 was detected in C/1995O1 (Hale-Bopp) for the first time, its abundance was less than 1/50 that of ammonia (Bockelée-Morvan et al. 2000). Therefore, it is assumed that all NH_2 is produced from ammonia through photodissociation by solar UV radiation in this study. The OPR of ammonia can be calculated from the observed OPR of NH_2 assuming photodissociation of ammonia to NH_2. The advantages for using NH_2 are;

(a) the strong NH_2 emission bands usually recognized in visible spectra for a comet at around 1 astronomical units (AU) from the Sun,

(b) NH_2 molecules mainly exist further from the nucleus than ammonia where the coma is optically thin, and

Table 4.1: Relevant observational parameters.

	C/1999S4 (LINEAR)	C/2001A2 (LINEAR)
Date (UT)	2000 July 5.58	2001 July 27.56
Heliocentric distance	0.863 AU	1.402 AU
Heliocentric velocity	-15.3 km s^{-1}	23.7 km s^{-1}
Geocentric distance	0.823 AU	0.467 AU
Geocentric velocity	-63.3 km s^{-1}	23.5 km s^{-1}
Total exposure time	1200 s	3600 s
Slit size	8.0 arcsec $\times$ 1.2 arcsec *1	7.0 arcsec $\times$ 1.0 arcsec *1
Spectral resolution ($\lambda/\Delta\lambda$)	30000	36000
Wavelength coverage	5100 — 7800 Å	5100 — 7800 Å

*1 The slit was put on the optical center of the comet.

(c) collisions between NH_2 and water can be neglected in the outer part of coma.

The first advantage leads to high S/N spectra of NH_2 while the last two simplify modeling the emission from NH_2 in the coma and translating the observed emission line strengths into the OPR.

4.2 Observations of Comet C/1999S4 (LINEAR) and Comet C/2001A2 (LINEAR)

In order to obtain high S/N emission lines of NH_2, my colleagues and I observed comet C/1999S4 (LINEAR) and comet C/2001A2 (LINEAR) with the Subaru telescope and the High Dispersion Spectrograph (HDS) (Noguchi et al. 1998). Observational parameters for these comets are listed in Table 4.1.

Both comets were discovered by the Lincoln Near Earth Asteroid Research (LINEAR) program (Stokes et al. 2000). It is thought that these comets came from the Oort cloud from the viewpoint of their orbits. These comets became bright near the perihelion passages and it was easy to get high-S/N spectra for the comets. C/1999S4 (LINEAR) approached its perihelion in late July 2000 and then disintegrated into many fragments (Weaver et al. 2001). This event was a precious chance to get the information of interior of the comet. Our observation was performed in early July 2000 before the disintegration occurred. On the other hand, C/2001A2 (LINEAR) showed a dramatic outburst of about 4 magnitudes at 1.3 AU

inbound. Our observation was performed when the comet was at 1.4 AU in post perihelion passage. Because this comet had a very high gas-to-dust ratio, high S/N spectra of gaseous emission lines could be obtained due to less influence by reflected sunlight caused by cometary dust grains. Thus, the cometary spectra at 0.86 AU and 1.40 AU from the Sun are available for the study. The spectra at different heliocentric distance can be used to check the validity of model calculations. Since the input solar flux is proportional to R_h^{-2}, the pumping rate from the ground state to upper electronic states is about 3 times larger in the case of C/1999S4 (LINEAR) than that in the case of C/2001A2 (LINEAR). As pointed out by Glinski et al. (2001), the population distribution in the ground state $\tilde{X}(0,0,0)$ is controlled by a balance between the pumping rate from the ground state to upper excited states and a radiative cooling rate in $\tilde{X}(0,0,0)$. The significant change in the input solar flux gives a severe examination for the model.

The NOAO IRAF software package with the standard reduction procedures was used here. The sensitivity calibration for instrument was performed as follows. The cometary spectrum was normalized by the continuum (which is reflected sunlight by cometary dust grains). Then the normalized spectrum was divided by normalized solar spectrum (Kurucz et al. 1984). The result was multiplied by the product of the solar spectrum and the albedo of the dust grains determined from the low dispersion spectra.

The albedo of cometary dust grains is typically about 10 % / 1000Å, and there are variations in it (Jewitt & Meech 1986). For C/1999S4 (LINEAR) the albedo of dust grains is assumed to be 15 % / 1000Å which is determined from a low dispersion spectroscopic observation carried out on 6 July 2000 (UT) by Fujii (2000). For C/2001A2 (LINEAR), the albedo is determined from a low dispersion spectrum taken on 12 July 2001 (UT) by 65cm telescope and the low dispersion spectrograph (see Figure 3.1). The albedo is 4.3 % / 1000Å for the comet.

Then, the final cometary spectrum is relatively calibrated with respect to the sensitivity of instrument. From the calibrated spectrum, four emission bands of NH_2, usually noted as (0,10,0), (0,9,0), (0,8,0) and (0,7,0) (Kawakita et al. 2001, Kawakita et al. 2000) can be extracted. These spectra are shown in Figure 4.1 and 4.2.

As described in Chapter 3, NH_2 (0,9,0) and (0,7,0) bands are suitable for fitting between observation and model spectrum. The S/N ratios of these

bands are high enough for comparing with model results. Furthermore, there is less contamination by other cometary gaseous species and less telluric absorption lines in these wavelength regions.

4.3 Results

Many ortho- and para- lines are resolved in the observed spectra. The OPR of NH_2 can be determined from these lines based on the fluorescence model calculations. Table 4.2 shows the emission lines measured and used for determination of OPR of NH_2. Please note that the designations for F_1 and F_2 levels were not included in this table. Since the spectral resolving power in the case of C/2001A2 (LINEAR) is higher than the case of C/1999S4 (LINEAR), some of listed lines are resolved in the spectrum of C/2001A2 (LINEAR) only. Unresolved lines are not measured in the case of C/1999S4 (LINEAR). The emission lines that had S/N ratios higher than $\approx$ 20 are measured here.

The sensitivity calibration of the spectra may be incomplete because the calibration was performed based on the measured albedo (color) of dust grains on the date different from the HDS observation for each comet. Therefore, the OPR values were estimated for (0,9,0) band and (0,7,0) band individually. Due to the narrow wavelength range of each band, smaller than 100 Å, the influence of error in measured color of dust grains is thought to be negligible within a certain band.

As the result of least χ^2 fitting for the lines in (0,9,0) band, the derived OPRs of NH_2 are 3.32$\pm$0.09 for C/1999S4 (LINEAR) and 3.43$\pm$0.09 for C/2001A2 (LINEAR), respectively. The error-bars are corresponding to 1-σ. The OPRs derived from (0,7,0) band are consistent with above results for each comet. However, these values depend on 0_{00}–1_{10} line in (0,7,0) band. Namely, when 0_{00}–1_{10} line is eliminated from the least χ^2 fitting, the obtained OPR is slightly different from the case including 0_{00}–1_{10} line. For comet C/1999S4 (LINEAR), OPR of 3.07$\pm$0.22 and 3.42$\pm$0.25 are obtained for the case including and excluding 0_{00}–1_{10} line, respectively. For comet C/2001A2 (LINEAR), obtained OPR values are 3.25$\pm$0.08 and 3.08$\pm$0.08 for the cases including and excluding the line, respectively. This is doubtful that 0_{00}–1_{10} line is contaminated by other unidentified lines. In fact, the profile of this line is not similar to a simple Gaussian function and asymmetric with respect to the central wavelength of the line. The asymmetric line profile of 0_{00}–1_{10} is shown in Figure 4.3 with the forbidden

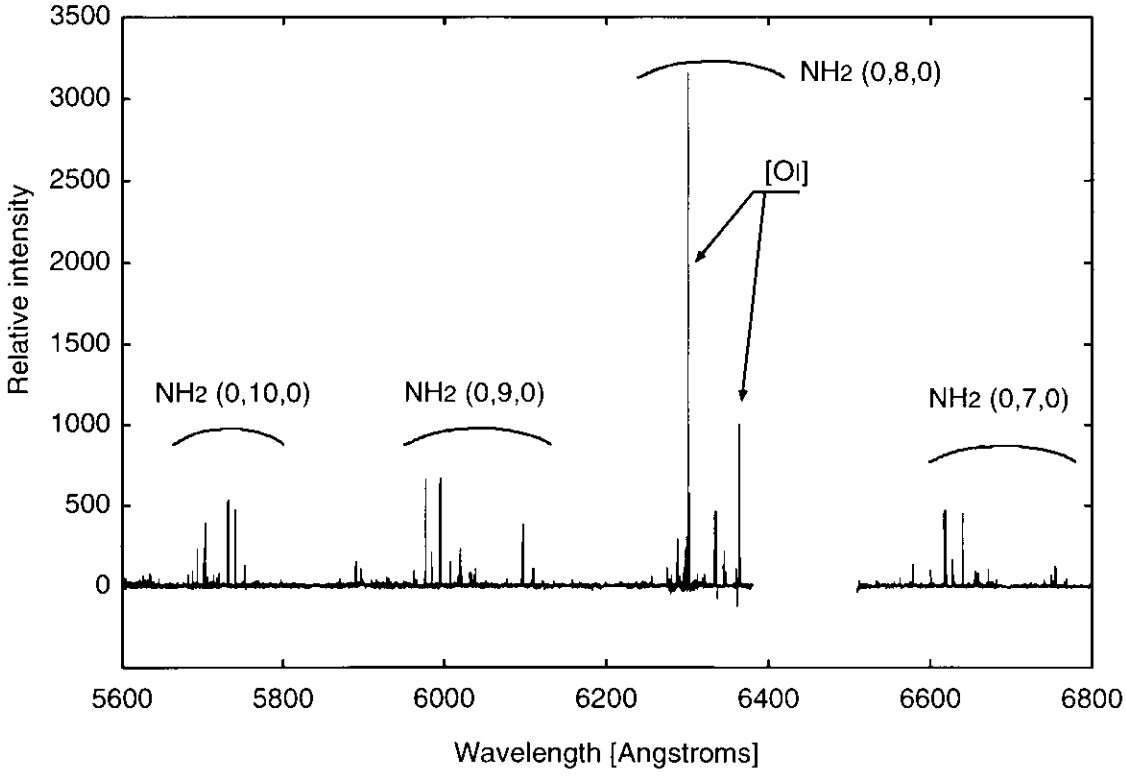

Figure 4.1: Observed spectra of NH_2 emission bands in comet C/1999S4 (LINEAR) on 2000 July 5 (UT). Wavelength region includes NH_2 (0,10,0), (0,9,0), (0,8,0), and (0,7,0) bands. The continuum component (the reflected sunlight by cometary dust grains) has been subtracted. The Doppler shift caused by cometary motion relative to the Earth has been corrected. In (0,8,0) band, there are two strong emission lines by forbidden transitions of atomic oxygen (at 6300 and 6364 Å).

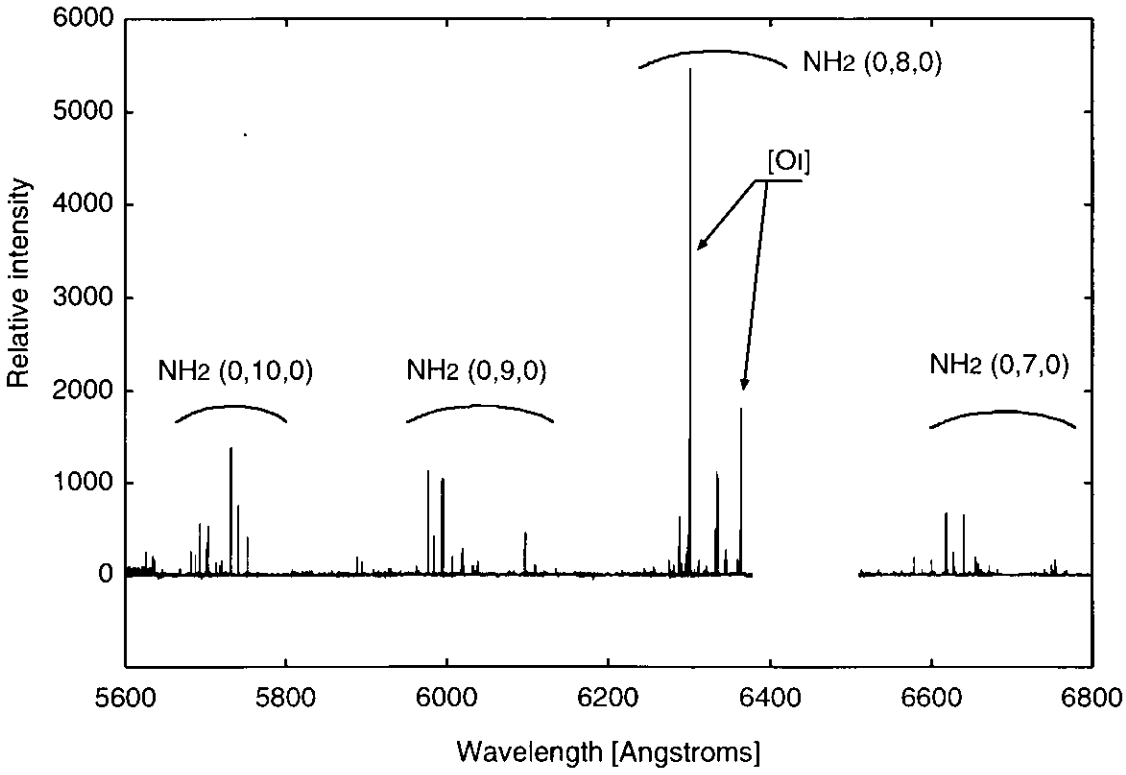

Figure 4.2: Same as Figure 4.1, but for comet C/2001A2 (LINEAR) on 2001 July 27 (UT).

Table 4.2: List of measured lines of NH_2.

Line assignment[*1]	Wavelength	C/1999S4[*2]	C/2001A2[*2]
(0,9,0) 3_{03}–2_{11} (o)	5962.6 Å	1352.53 (30.6)	1223.6 (33.6)
(0,9,0) 2_{02}–1_{10} (p)	5965.2 Å	618.0 (27.5)	591.14 (32.8)
(0,9,0) 1_{01}–1_{11} (o)	5976.4 Å	8517.3 (29.6)	12813.3 (33.6)
(0,9,0) 2_{02}–2_{12} (p)	5976.9 Å	——	2866.0 (31.3)
(0,9,0) 3_{03}–3_{13} (o)	5977.2 Å	——	3360.0 (34.3)
(0,9,0) 0_{00}–1_{10} (p)	5984.6 Å	2777.29 (30.6)	4912.8 (36.2)
(0,9,0) 1_{01}–2_{11} (o)	5995.0 Å	8567.1 (29.6)	11983.4 (34.6)
(0,9,0) 2_{02}–3_{12} (p)	6007.0 Å	2100.6 (31.2)	2264.34 (37.7)
(0,9,0) 3_{21}–2_{11} (o)	6017.4 Å	828.24 (27.6)	686.91 (32.1)
(0,9,0) 3_{21}–2_{11} (o)	6018.7 Å	2515.59 (29.6)	2576.7 (32.1)
(0,9,0) 2_{21}–1_{11} (o)	[*3]		
(0,9,0) 3_{03}–4_{13} (o)	6020.0 Å	——	2255.5 (35.0)
(0,9,0) 2_{20}–1_{10} (p)	6022.1 Å	747.6 (26.1)	1102.38 (30.5)
(0,9,0) 3_{21}–3_{13} (o)	6033.6 Å	1061.06 (26.7)	1065.46 (29.5)
(0,9,0) 2_{20}–2_{12} (p)	6034.0 Å	562.1 (26.7)	526.26 (28.8)
(0,9,0) 2_{21}–2_{11} (o)	6037.5 Å	981.12 (27.9)	1113.4 (27.4)
(0,9,0) 2_{21}–2_{11} (o)	6039.2 Å	1310.75 (28.5)	1559.8 (29.5)
(0,7,0) 1_{01}–1_{11} (o)	6618.0 Å	5307.2 (20.9)	6700.2 (25.2)
(0,7,0) 2_{02}–2_{12} (p)	6618.7 Å	1390.48 (19.1)	1610.28 (22.6)
(0,7,0) 3_{03}–3_{13} (o)	6619.3 Å	1996.96 (19.8)	1860.47 (23.7)
(0,7,0) 0_{00}–1_{10} (p)	6627.9 Å	1874.5 (18.0)	2594.4 (22.4)
(0,7,0) 1_{01}–2_{11} (o)	6640.7 Å	5194.0 (19.8)	6599.6 (24.7)
(0,7,0) 2_{21}–1_{11} (o)	6654.6 Å	484.12 (16.4)	769.86 (19.8)
(0,7,0) 2_{02}–3_{12} (p)	6655.6 Å	——	1219.69 (22.4)
(0,7,0) 2_{21}–1_{11} (o)	6659.2 Å	959.4 (20.5)	1100.0 (18.7)
(0,7,0) 2_{20}–1_{10} (p)	6661.4 Å	267.36 (15.0)	496.48 (18.7)

[*1] Ortho-NH_2 lines are indicated by 'o' and para lines by 'p'.

[*2] Measured flux of the line is in arbitrary units for each comet. 1σ error is in parenthesis.

[*3] This is blended with (0,9,0) 3_{21}–2_{11}.

transition of atomic oxygen at 5577 Å which is a transition between singlet levels. Since the line profile of atomic oxygen at 5577 Å is symmetric like a Gaussian function, the asymmetry recognized in 0_{00}–1_{10} line is not caused by the instrumental line profile. Although 0_{00}–1_{10} line should be split into two lines due to a net electron spin of NH_2 for a higher spectral resolution, the line profile indicated that the observed line seems to consist of three lines (these lines can not be separated clearly in the observed spectra). These facts support that the line is contaminated by other unidentified emission line.

In this thesis, the final value of OPR is derived just from (0,9,0) band, which has no concern both for the S/N and for the contamination by unidentified lines. The (0,7,0) band is used to check the consistency of the final values of OPR derived from (0,9,0) band.

The modeled spectra for (0,10,0), (0,9,0), (0,8,0), and (0,7,0) bands are shown in Figure 4.4 and 4.5 which can reproduce the observed spectra well. The perturbation effect is recognized for a few lines marked by 'p' in the Figures (the perturbation is not included in the calculation). The forbidden lines of atomic oxygen are not included in the calculation of (0,8,0) band. The unidentified emission lines (UID) are marked by 'u', which consistent with high-dispersion spectra ever observed (Brown et al. 1996, Morrison et al. 1997, Zhang et al. 2001). Brown et al. (1996) proposed that these UID lines caused by high-J rotational levels of NH_2. Biesner et al. (1989) showed that NH_2 generated from ammonia is excited to high rotational levels in a vibronic ground state $\tilde{X}$(0,0,0) just after ammonia photodissociated. Such high excited rotational levels are not included in the present model calculation.

As discussed above, it is safely assumed that NH_2 is produced from ammonia by photodissociation due to solar ultraviolet radiation. The permutation group theory (Quack 1977, Longuet-Higgins 1963) is applied to a whole reaction system including a source molecule NH_3 and products NH_2 and H. The theory predicts that only ortho-NH_2 is generated from ortho-NH_3, and both the 1:1 ratio product of ortho- and para-NH_2 from para-NH_3. This prediction is supported by an experimental study in the laboratory (Fuke et al. 1988). As a result, the OPRs of cometary ammonia are determined to be 1.16±0.05 for C/1999S4 (LINEAR) and 1.22±0.05 for C/2001A2 (LINEAR), respectively.

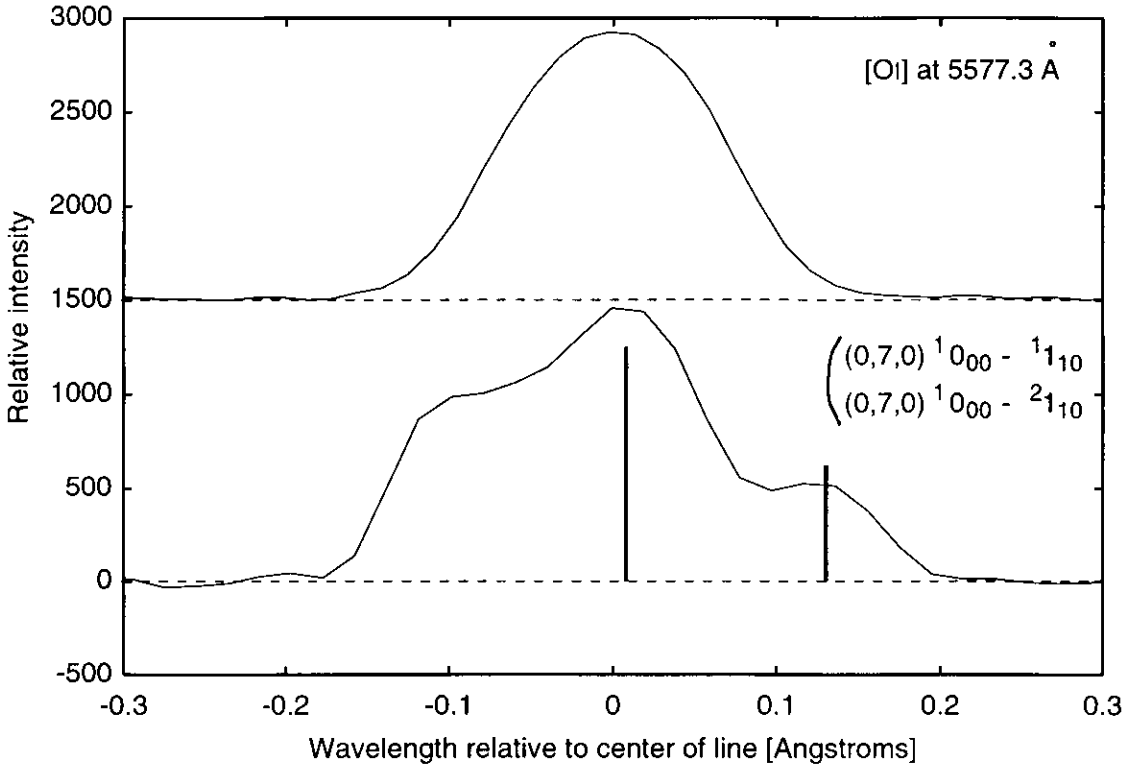

Figure 4.3: Line profiles of the forbidden transition of atomic oxygen (at 5577 Å) and NH_2 (0,7,0) 0_{00}–1_{10} line in C/2001A2 (LINEAR). The line profile of atomic oxygen is symmetric relative to the line center. On the other hand, 0_{00}–1_{10} line seems to consist of three components of emission lines. Two of them are identified as fine structure of 0_{00}–1_{10} line (expected intensities are shown in the figure). One additional line is thought to be an unidentified line.

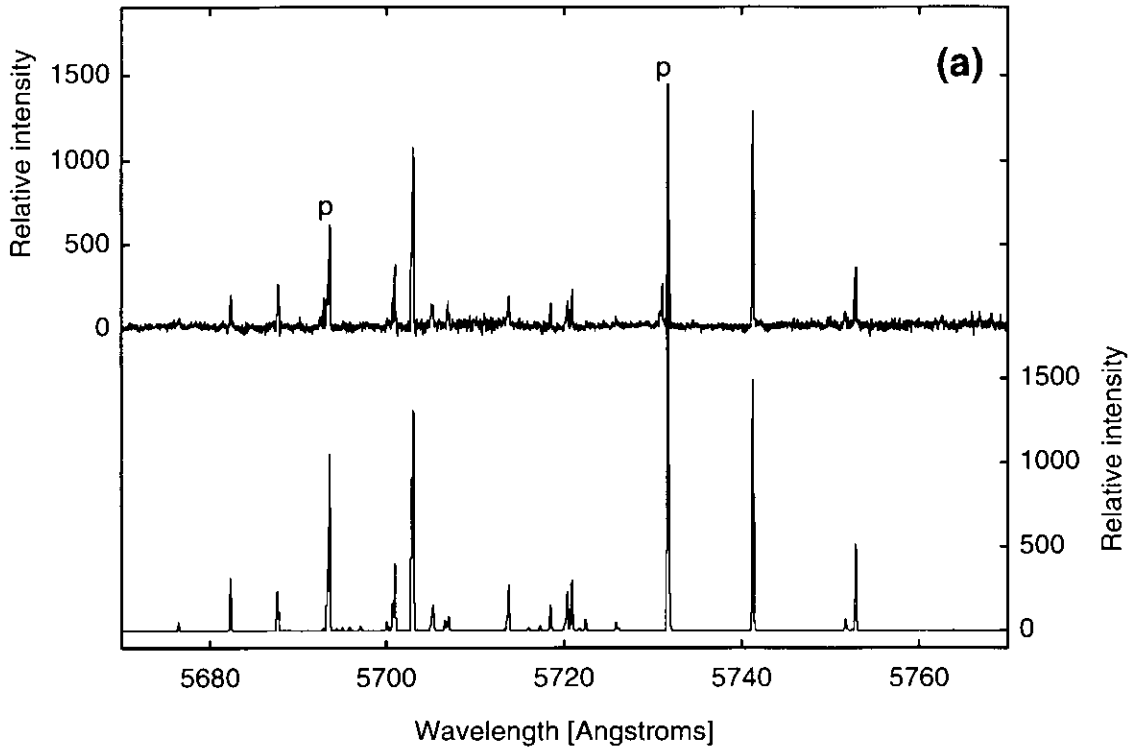

Figure 4.4: Observed (top) and calculated (bottom) spectra of NH_2 emission bands in comet C/1999S4 (LINEAR) on 2000 July 5 (UT). a) (0,10,0) band, b) (0,9,0) band, c) (0,8,0) band, and d) (0.7,0) band. The effect of perturbation is shown for a few lines in observed spectrum (marked by 'p'), and several unidentified lines exist (marked by 'u'). In (0,8,0) band, there are strong emission lines of forbidden transitions of atomic oxygen (at 6300 and 6364 Å) only in observed spectrum.

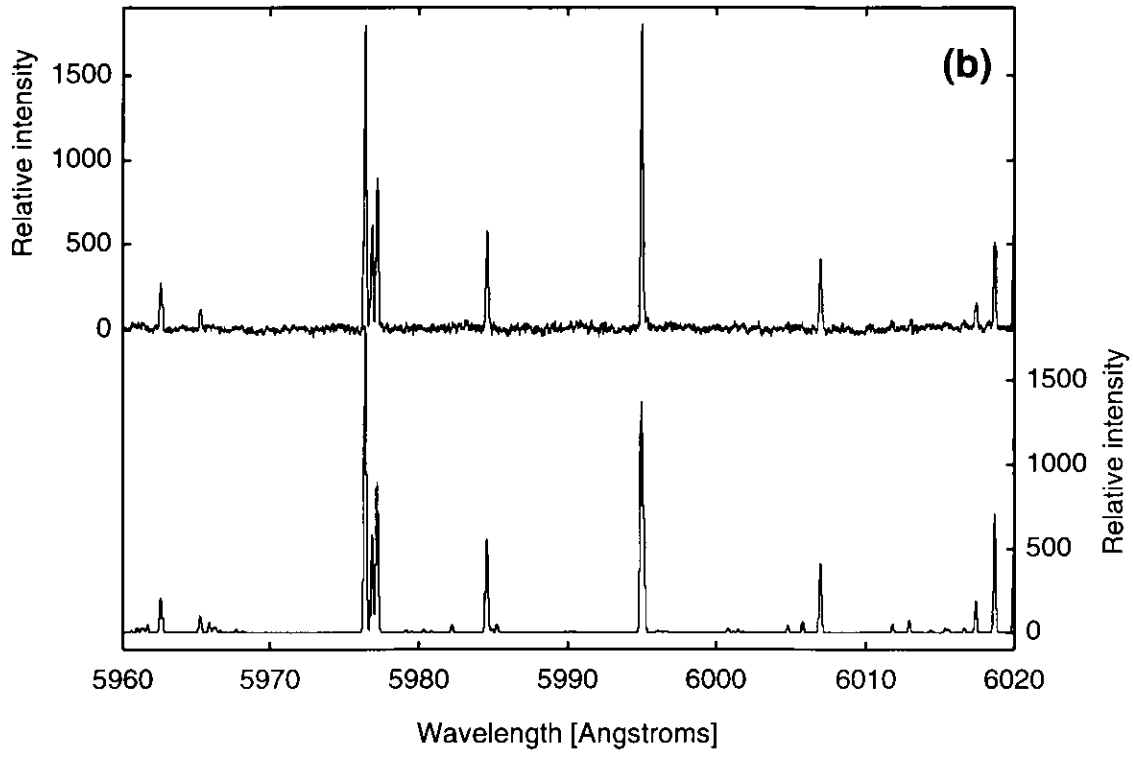
(b)
Relative intensity
1500
1000
500
0
1500
1000
500
0
Relative intensity
5960
5970
5980
5990
6000
6010
6020
Wavelength [Angstroms]

Continued.

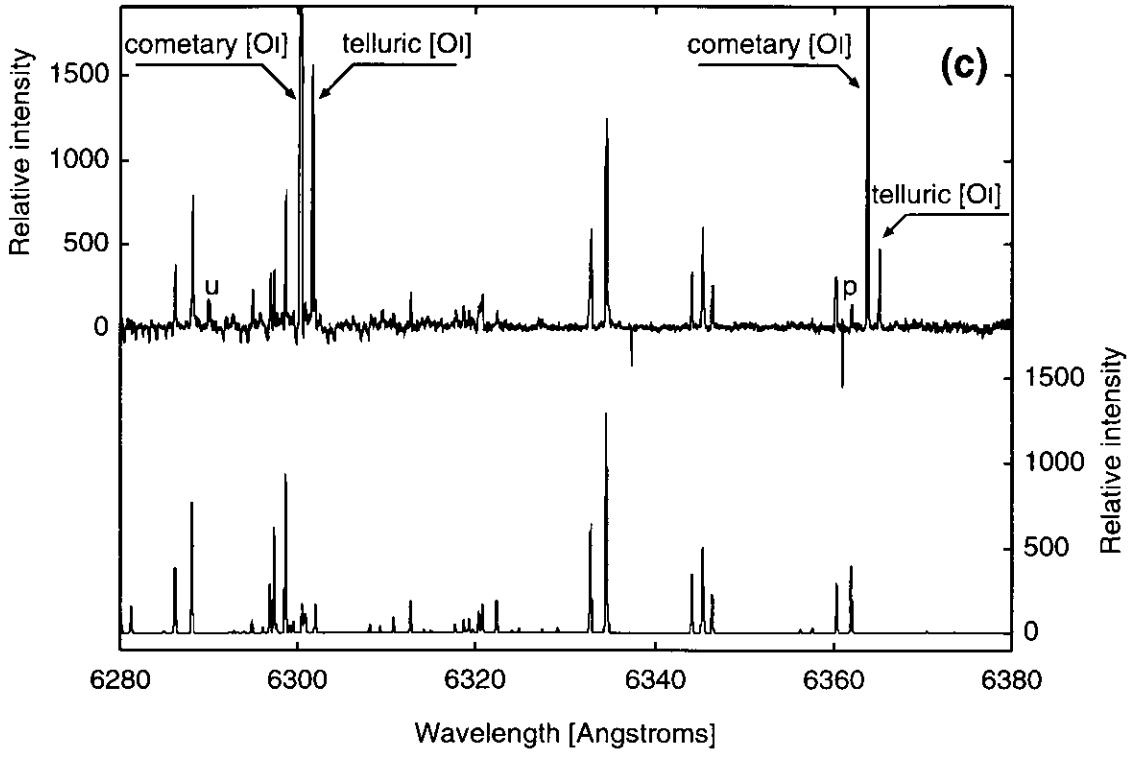
cometary [OI]
telluric [OI]
cometary [OI]
(c)
telluric [OI]
u
p
Relative intensity
1500
1000
500
0
6280
6300
6320
6340
6360
6380
Wavelength [Angstroms]

Continued.

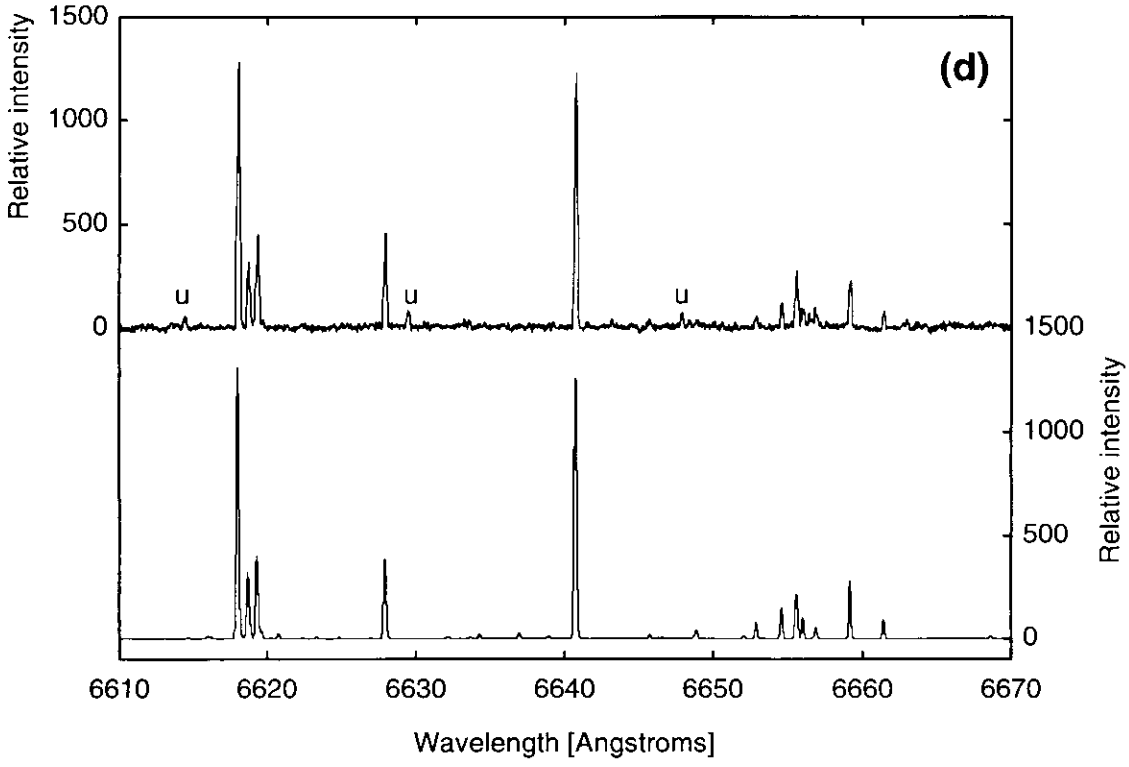
(d)
Relative intensity
1500
1000
500
0
u
u
u
1500
1000
500
0
Relative intensity
6610
6620
6630
6640
6650
6660
6670
Wavelength [Angstroms]

Continued.

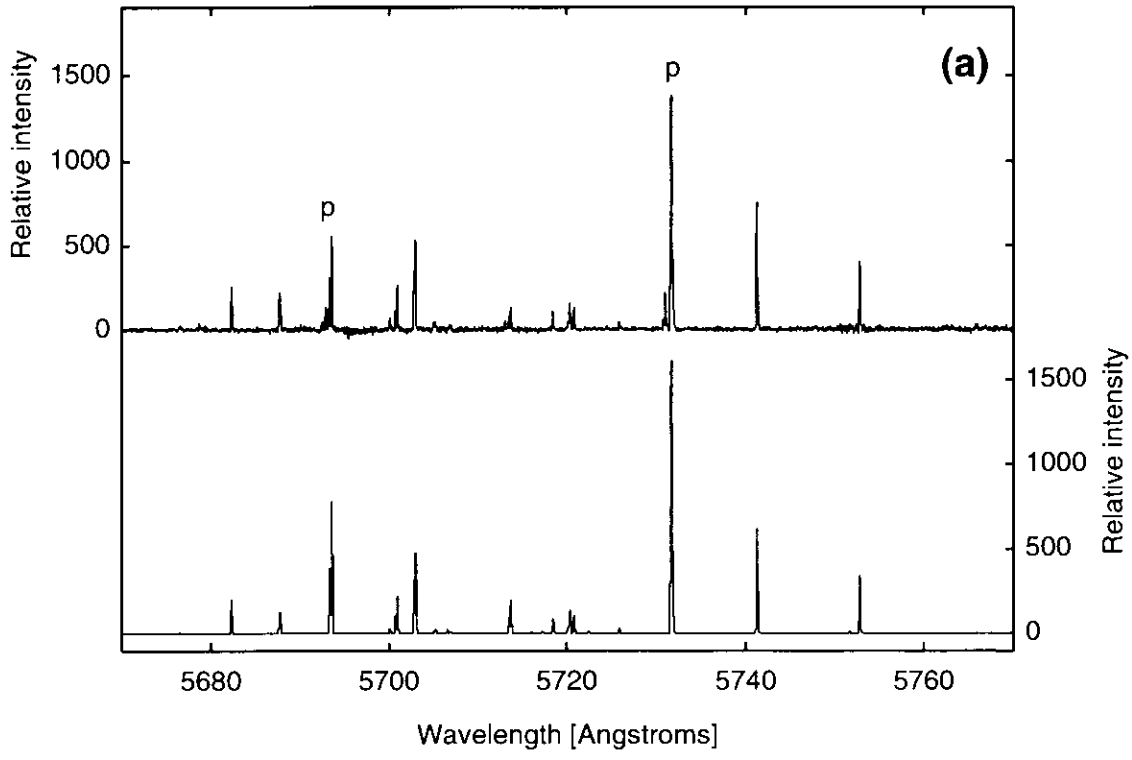

Figure 4.5: Same as Figure 4.4, but for comet C/2001A2 (LINEAR) on 2001 July 27 (UT).

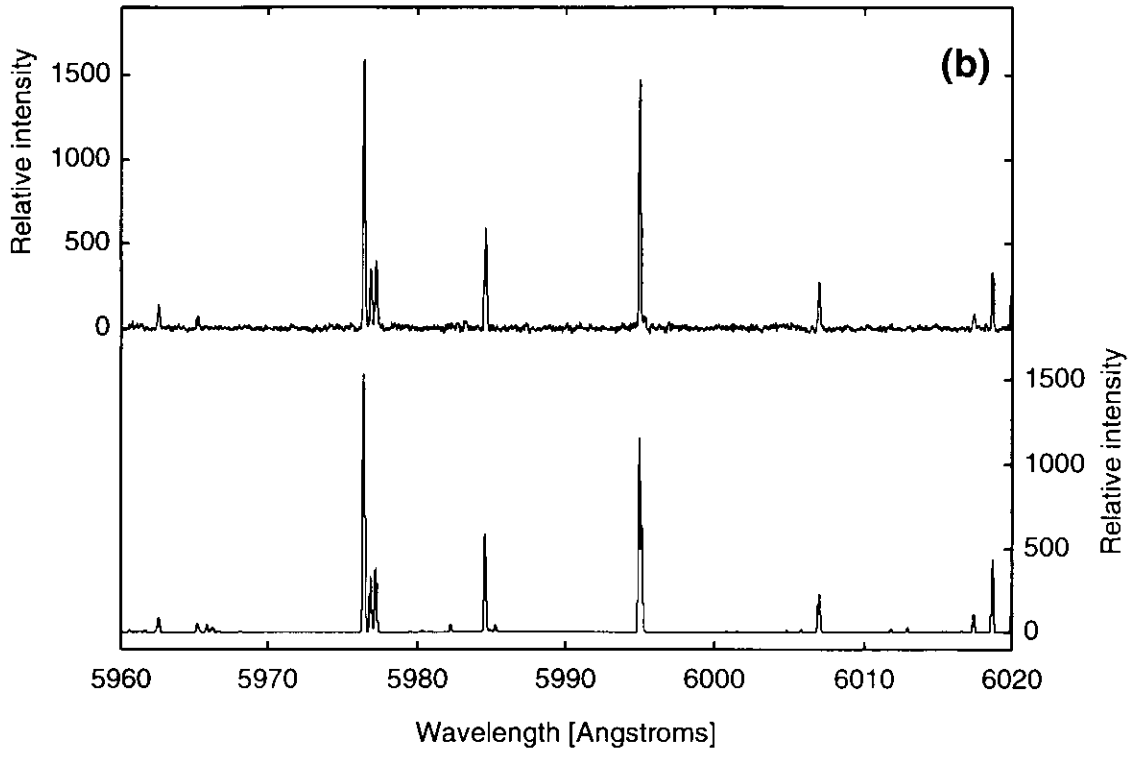
(b)
Relative intensity
1500
1000
500
0
1500
1000
500
0
Relative intensity
5960
5970
5980
5990
6000
6010
6020
Wavelength [Angstroms]

Continued.

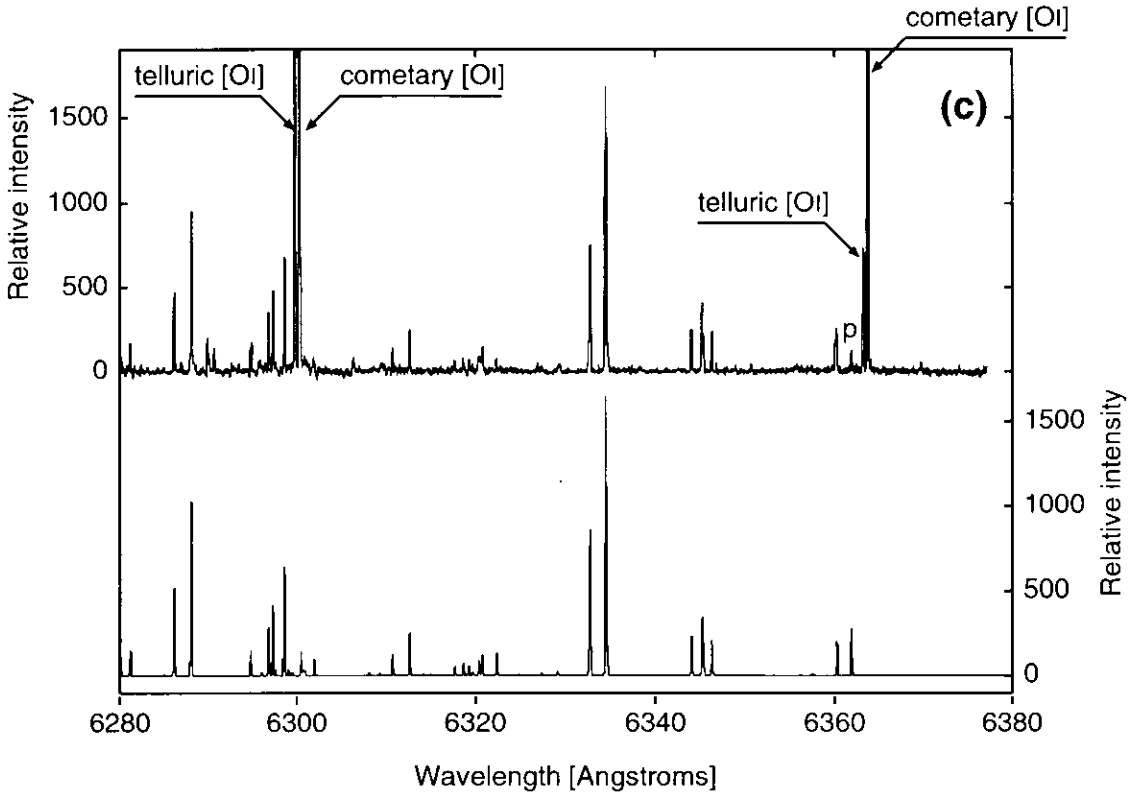
cometary [OI]
telluric [OI]
cometary [OI]
(c)
telluric [OI]
p
Relative intensity
1500
1000
500
0
6280
6300
6320
6340
6360
6380
Wavelength [Angstroms]

Continued.

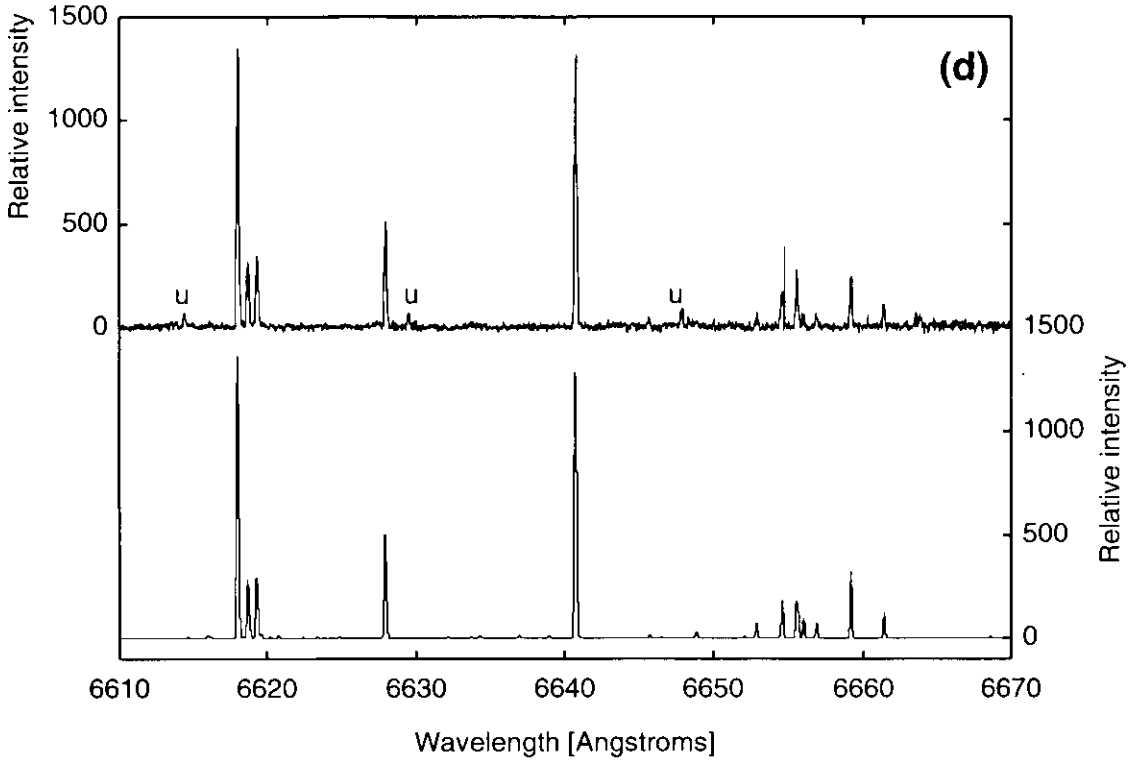
(d)
Relative intensity
1500
1000
500
0
u
u
u
1500
1000
500
0
Relative intensity
6610
6620
6630
6640
6650
6660
6670
Wavelength [Angstroms]

Continued.

4.4 Discussion

The OPR of ammonia can be calculated for a given spin temperature based on the molecular constants of ammonia (Poynter & Kakar 1975). Figure 4.6 shows the OPR of ammonia with respect to a spin temperature. The OPR of ammonia approaches 1.0 if ammonia ice formed and equilibrated under the high-temperature conditions ($\geq$ 40 K) while it becomes larger under the low-temperature conditions (e.g., more than 10 at 5 K). The OPRs derived here indicated the spin temperatures of 28^{+3}_{-2} K and 26^{+2}_{-1} K for comet C/1999S4 (LINEAR) and C/2001A2 (LINEAR), respectively. The spin temperatures of ammonia in both comets C/1999S4 (LINEAR) and C/2001A2 (LINEAR) are consistent with the spin temperature of water ever observed in Oort cloud comets (comet C/1995O1(Hale-Bopp) and comet 1P/Halley).

Mumma et al. (1993) and Crovisier (1999) argued that the OPR could reflect the temperature at the moment of formation or condensation of the molecules. The results shown here exclude the high temperature limit (OPR = 1 for ammonia). This fact eliminates the formation of cometary ammonia through chemical reactions only in gas phase (e.g., reactions shown in Hiraoka et al. 1995). Because the chemical reactions in gas phase are exothermal, the OPR of ammonia formed in the gas phase should be unity according to the nuclear spin statistical weights of the ortho and para species (Irvine 1999). The OPR smaller than the high temperature limit indicates the formation in the low temperature conditions. Saito et al. (2000) suggested that a part of ammonia in cold dark clouds could originate from dust related reactions associated with energetic events. Dust related reactions were also suggested by Dickens & Irvine (1999) for the formaldehyde (H_2CO) in dark clouds. Thus, the formation of ammonia on the cold grain surface demonstrated by Hiraoka et al. (1995) seems to be important. It appears that ammonia was produced through the gas–grain chemistry in the pre-solar molecular cloud or in the solar nebula, in which ammonia formed on the icy mantle of grains (Hiraoka et al. 1995). In this case, the OPR of ammonia may reflect the temperature of icy grains where the molecules formed (Irvine 1999). Alternatively, ammonia formed in the gas phase (with OPR = 1) and then frozen onto cold grains that contain paramagnetic species or magnetic nuclei could undergo ortho-para conversion in a relatively short time (cf. Momose et al. 1997). The OPR of ammonia re-equilibrated according to the low temperature of icy grains

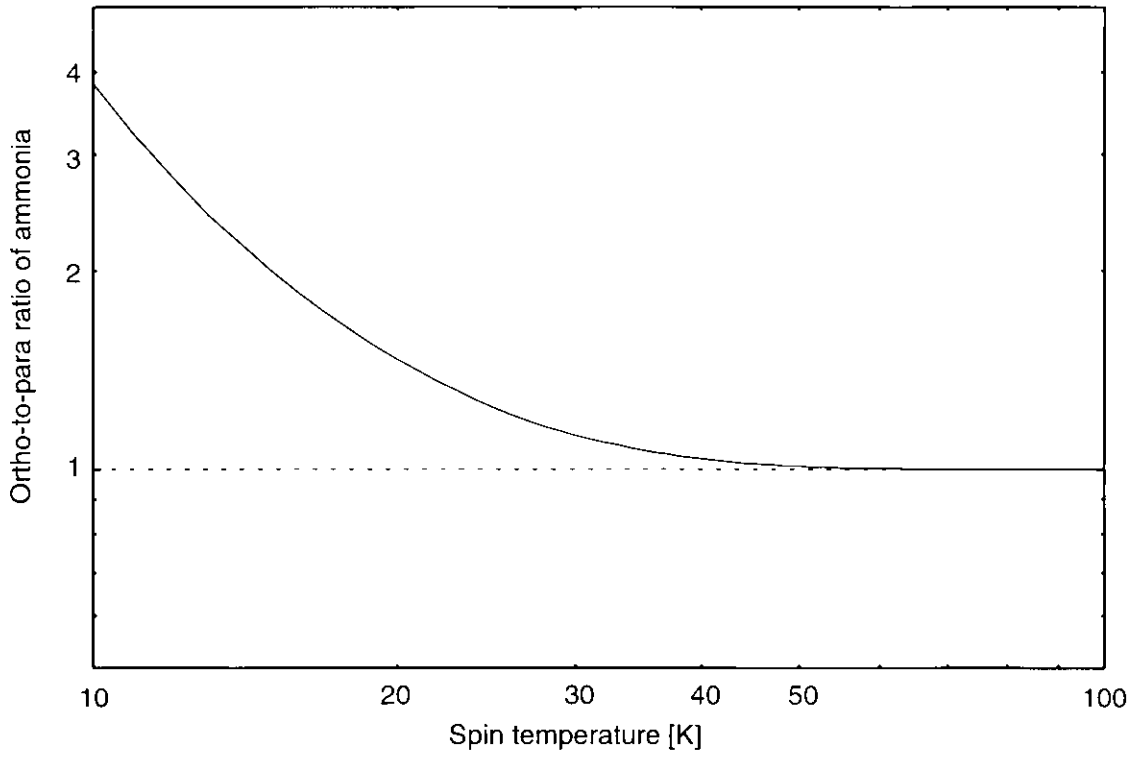

Figure 4.6: Ortho-to-para ratio of ammonia with respect to a spin temperature. Ammonia is a good probe for investigating a temperature up to 40 K. For more than 50 K the OPR of ammonia is close to unity (its high temperature limit).

in this case. Although such ortho-para conversion process is studied in laboratory, the possibility of ortho-para conversion in cometary nuclei is not yet clear because we don't know in detail about the conditions (especially, the temperature) of interior of cometary nuclei and about the cometary icy grain (its structure, composition, and so on.). Therefore, a sample return mission for cometary grains in the future (e.g., STARDUST mission) and a laboratory investigation of ortho-para conversion mechanisms for ammonia under cometary conditions are required. Anyway, in either case, the OPR less than 1 for ammonia is indicative of grain processing.

The spin temperature of ammonia which is consistent with that of water, $\approx$ 30 K, indicates that the ammonia and water ices formed under the same temperature condition. This fact supports the scenario that ammonia and water ices formed or condensed on the icy grains at a certain temperature. This consistency is important for investigations on the molecular formation processes in the successive stages from the molecular cloud to protoplanetary disk. The next question is when and where the molecules formed during the period from the pre-solar cloud to the solar nebula.

One may think that the OPR re-equilibrated in the interior of cometary nucleus during the long storage time ($\approx$ 4.5 Gyr) in Oort cloud or in Kuiper belt after the solar system formed as argued by Mumma et al. (1993). However, Irvine et al. (2000) pointed out that the orbital periods for the comets in which the spin temperatures of water were ever measured span the range from 4000 to 6 years, so it seems very unlikely that all these comets would have internal temperatures near 30 K. A comet with longer orbital period seems to have a lower internal temperature because its aphelion distance is further from the Sun. The additional results for spin temperatures of ammonia also supports this idea. C/1999S4 (LINEAR) has tremendously longer orbital period than 4000 years. Thus, the re-equilibration of OPR in a cometary nucleus during its long stay in Oort cloud or in Kuiper belt seems to be impossible. If the re-equilibration of OPR of ammonia occurred under the lower temperature conditions, the OPR would be larger for ammonia, e.g., more than 4 corresponding to $\leq$ 10 K (see Figure 4.6).

In contrast with above discussion, the OPR might re-equilibrate quickly and reflect the temperature just before the sublimation from cometary ice. The typical sublimation equilibrium temperatures of pure water ice and pure ammonia ice under cometary conditions are 152 K and 78 K, respectively (cf. Crovisier & Encrenaz 2000). These values are for equilibrium

between the relevant ice and its own vapor. The sublimation temperatures are quite different for a mixture of ices. Because highly polar molecules like NH_3 has strong affinity for water, it is expected that water retains the ammonia for the case of cometary ice (which is a mixture of water, ammonia and so on.). Therefore the sublimation temperature would be higher than that of the pure ammonia ice (cf. Crovisier & Encrenaz 2000). Thus, the temperature range of sublimation is much higher than the spin temperature in the case of ammonia (and in the case of water). It seems unlikely that the OPR might re-equilibrate to $\approx$ 30 K for both ammonia and water in the cometary nuclei. Laboratory studies of ortho-para conversion rate under cometary conditions are required for further discussions on the ortho-para conversion in cometary nuclei.

Irvine et al. (2000) proposed the possibility that the cometary OPR might be reset in the coma where near-nucleus temperatures drop to $\approx$ 30 K and proton transfer reactions can occur with H^+ and H_3O^+. However, the spin temperatures obtained for water and ammonia so far can reject this hypothesis because the kinetic temperature at the near nucleus coma depends strongly on the input solar flux, a production rate of gaseous molecule, a gas-to-dust ratio, and so on (Combi et al. 1997b). It is difficult to agree that all comets in which spin temperatures were determined for water or ammonia had the same kinetic temperature near the nucleus region at the observations. Moreover, the lowest kinetic temperature in the coma calculated by Combi et al. (1997b) is quite lower than the spin temperature determined for water in the case of comet C/1995O1 (Hale-Bopp). Thus, the reset of OPR in the coma can be rejected.

It should be noted that Irvine (1999) concluded that clearly both further observations and laboratory studies of ortho-para interchange are needed before the cometary results can be interpreted. The experiments for the spin relaxation in an environment similar to the interior of cometary nucleus should be investigated in the future. In the following part, however, the conditions of molecular formation are discussed based on the comparisons between studies on the temperatures at which cometary molecules formed and/or processed.

The temperature ranges regarding to the formation of cometary molecules are summarized in Table 4.3. The spin temperatures of cometary ammonia shown here are consistent with temperatures determined for comet C/1995O1 (Hale-Bopp) from D/H ratios of water and hydrogen cyanide (Blake et al. 1999, Meier et al. 1998a, 1998b). Bergin et al. (1999)

Table 4.3: Temperatures related to cometary formation.

Temperature	Remarks	References
26 — 28 K	Spin temperatures of ammonia.	This work.
25 — 35 K	Spin temperatures of water.	Crovisier (1999), Mumma et al. (1993).
> 30±10 K	D/H ratio in water and hydrogen cyanide for entire coma.	Meier et al. (1998a, 1998b).
20 — 30 K	D/H ratio in water and hydrogen cyanide in jets.	Blake et al. (1999).
25 — 40 K	[HDO]/[H_2O] and [CO_2]/[H_2O].	Bergin, Neufeld, & Melnick (1999).
< 35 — 40 K	Possible enhancement of argon.	Stern et al. (2000).
> 20 — 25 K	Depletion of neon.	Krasnopolsky et al. (1997), Stern et al. (2000).

suggested the possible formation of molecules in the pre-solar cloud and the solar nebula at ≈ 25 — 40 K. Recent detection of argon in comet C/1995O1 (Hale-Bopp) (Stern et al. 2000) requires that the interior of the comet has never been exposed to 35 — 40 K temperatures. If the argon also existed in the comets observed in this study, the formation regions of the comets are further restricted. Furthermore, the depletion of neon in comet Hale-Bopp may indicate the temperature range higher than 20 — 25 K (Krasnopolsky et al. 1997, Krasnopolsky & Mumma 2001, Stern et al. 2000). *These results are consistent with the formation of cometary molecules at the temperature of ≈ 30 K.*

If the Sun formed as an isolated low mass star in the dense core of dark cloud, the temperature of the dark cloud seems to be about 10 K (Langer et al. 2000). In this case, the obtained spin temperature of cometary ammonia which is consistent with other studies, seems to be higher than the expected temperature in pre-solar molecular cloud. Therefore, the spin temperature of ammonia, about 30 K, is thought to be a temperature at the place where the ammonia formed or condensed in the solar nebula. If it is assumed that the cometary molecules formed or re-processed in the solar nebula at a certain temperature condition, the formation zone of the comets can be inferred from the observations. The temperature distribution in the solar nebula was investigated by many researchers so far (e.g., Hersant et al. 2001, Aikawa et al. 1999, and Willacy et al. 1998). Although the temperature distribution depends on the physical model of solar nebula, the temperature of ≈ 30 K indicates the giant planets' region in the solar nebula in most cases. For example, the formation zone of both comets C/19999S4 (LINEAR) and C/2001A2 (LINEAR) is considered to be an area between the orbits of Saturn and Neptune (10 — 20 AU from the Sun) in the mid-plane of solar nebula based on the calculation of Willacy et

al. (1998). Comets C/1999S4 (LINEAR) and C/2001A2 (LINEAR) came from the Oort cloud which is thought to originate from the cometesimals formed in the giant planets' region based on the statistical studies on orbital evolutions of cometesimals (e.g. Weissman 1999). The formation zone inferred from spin temperatures is consistent with the area inferred from orbital evolutions.

In contrast with above case, the Sun might have been born in a region of high mass star formation (Irvine 1999, Goswami & Vanhala 2000), and the temperature of pre-solar cloud might be higher. In this case, the spin temperature of ammonia and the temperature range indicated by other studies may reflect the temperature of pre-solar molecular cloud (or the temperature at other stage of solar system formation). Of course, it might be a temperature in the solar nebula. Present data are not enough to distinguish these scenarios for our solar system. The further observations of OPRs of cometary ammonia may be able to give an answer to this question. Since the Kuiper belt comets (Jupiter family short period comets) formed in Kuiper belt region where was colder than the giant planets' region (a formation zone of Oort cloud comets), the spin temperatures of Kuiper belt comets will be lower than that of Oort cloud comets if the the spin temperature determined according to the place where comets formed in the solar nebula. On the other hand, if there are no significant difference in spin temperatures between Oort cloud comets and Kuiper belt comets, the spin temperature may indicate the temperature at a common place for the Oort cloud comets and Kuiper belt comets. There is only one sample of Kuiper belt comet in the case of water, and no samples for the ammonia case. Clearly more samples are needed for investigating a real meaning of OPR in cometary molecules. Further observations for OPR of cometary ammonia and statistical study based on more samples will also make clear some of unclear issues on OPR of cometary molecules pointed out by Irvine et al. (2000).

Finally, other observations for each comet observed in this study will be shown and compared with the result described above. For the case of C/1999S4 (LINEAR), there are many studies on it because it was bright and it disintegrated into many fragments (this comet gave a precious chance to know the information about interior of comet). It is reported that the highly volatile species such as CO, CH_4, and C_2H_6 were depleted in C/1999S4 (LINEAR) compared with the other Oort cloud comets which formed near the orbit of Neptune in the solar nebula (Mumma et al. 2001a,

Bockelée-Morvan et al. 2001). Mumma et al. (2001a) proposed the hypothesis that C/1999S4 (LINEAR) formed in the warmer region (5 — 10 AU from the Sun). The result shown here is inconsistent with the formation at such warmer place. It may be possible to explain this discrepancy by the scenario that the icy grains on which ammonia (and other cometary molecules) formed near the orbit of Uranus (T≈28K) migrated into inner region of solar nebula during an accretion phase of solar nebula and the highly volatile species sublimated from the ice (but the OPR of ammonia did not change), and then the cometary nucleus formed from the icy grains at the warmer place. As another possible explanation, since the solar nebula continuously cooled down and the temperature distribution of solar nebula changed in the protoplanetary disk phase (Hersant et al. 2001), the materials formed at the early stage of the protoplanetary disk phase might be processed in warmer environment even if in the far-off region of solar nebula. On the other hand, Farnham et al. (2001) reported the depletion in carbon chain molecules such as C_2 or C_3 observed in optical spectra in C/1999S4 (LINEAR) and possible formation of the comet in outer part of solar nebula (Kuiper belt region). However it is not clear whether the abundances of such carbon chain molecules are primordial or not (C_2 and C_3 are thought to be photodissociated products, not parent molecules). Note that the depletion in C_2 is consistent with the depletion in C_2H_6 reported by Mumma et al. (2001a) since C_2H_6 is a possible parent molecule of C_2 (cf. Crovisier & Encrenaz 2000).

For the case of C/2001A2 (LINEAR), there are only several preliminary reports yet. Mumma et al. (2001b) reported that C/2001A2 (LINEAR) was enriched in C_2H_6 which is a highly volatile molecule. Crovisier et al. (2001) also reported that the very volatile molecule, H_2S, was more abundant in C/2001A2 (LINEAR) than other comets. The derived spin temperature of ammonia for this comet, $\approx$ 26 K, is consistent with the enrichment in very volatile species such as C_2H_6 and H_2S. On the other hand, Feldman et al. (2001) reported that abundance ratio between Ar and O (Ar/O ratio) was more than a factor of ten less than solar abundance. This may indicate the formation of C/2001A2 (LINEAR) at warmer place of solar nebula ($>$ 35 — 40 K), or the comet had been exposed to such warmer temperature for long time.

As described in this section, the further observations of the OPRs of

cometary ammonia are strongly recommended for not only other Oort cloud comets but also the short period (Kuiper belt) comets. These observations may be able to reveal the meaning of OPRs. The variation of OPRs measured in comets is essentially important for the investigation on origin of solar system. The method of the OPR determination for cometary ammonia established in this study should be applied to other comets, in order to know the OPR variety if any.

4.5 Summary

In this chapter the new tool to investigate an OPR of cometary ammonia and the first applications of this method for the cases of comet C/1999S4 (LINEAR) and comet C/2001A2 (LINEAR) are shown. The OPRs of ammonia are derived to be 1.16±0.05 for C/1999S4 (LINEAR), and 1.22±0.05 for C/2001A2 (LINEAR), respectively. The results are corresponding to the spin temperatures of 28^{+3}_{-2} K and 26^{+2}_{-1} K for comet C/1999S4 (LINEAR) and C/2001A2 (LINEAR), respectively. These are consistent with OPRs of water in other comets ever observed. The OPR of ammonia excludes the high temperature limit and it can eliminate ammonia formation by reactions only in gas phase. Possible formation on grain surface, in icy grain mantle, is supported by results shown here. The temperature range shown here is corresponding to the temperature between the orbit of Saturn and that of Uranus in solar nebula if it is assumed that the spin temperature reflects the temperature where the molecules formed in the solar nebula. This region is thought to be a formation zone of the comets. This conclusion is consistent with the statistical studies based on the simulations of orbital evolution, e.g., Weissman (1999).

The temperature range suggested by D/H ratio water and hydrogen cyanide observed in comets and by the argon and neon abundances are also consistent with the temperature range obtained from ammonia in this study (see in Table 4.3). However, the abundance of highly volatile species in comet C/1999S4 (LINEAR) suggests the formation of the comet at warmer place (Mumma et al. 2001a). The depletion in argon for comet C/2001A2 (LINEAR) also suggests the formation at warmer place (Feldman et al. 2001). These discrepancies should be investigated from the viewpoints of both observations and chemical models.

Using the method shown in this chapter, OPRs of ammonia for other comets will be able to be determined from high-dispersion optical spectra

of the comets in the future. Especially the comparison between OPRs of ammonia for Oort cloud comets and Kuiper belt comets, is important for investigating the formation region of these comets.

Chapter 5

Conclusion

In this thesis a new method to investigate OPR of cometary ammonia from NH_2 radicals is developed from the viewpoint of photodissociation of ammonia to NH_2.

In Chapter 2, the NH_2 spatial distribution in comet C/1996B2 (Hyakutake) is studied using the technique of Collisional Monte Carlo simulation. The low dispersion spectrum could be obtained in the coma near nucleus region where the brightness spatial profile of NH_2 is sensitive to properties of its parent molecules. On the basis of the comparison between model results and the observation, it is confirmed that NH_2 is produced directly from cometary ammonia through the photodissociation by solar ultraviolet radiation. Based on the assumption of NH_2 generation from ammonia by a photodissociation, the OPR of ammonia can be determined from OPR of NH_2.

In Chapter 3, the fluorescence excitation model of NH_2 is developed. Using this model, the emission spectra of NH_2 can be calculated and be compared with actual high-dispersion spectra of NH_2 in optical region. Usually it is not so difficult to get high-S/N ratio spectra of NH_2 for comets around 1 AU from the Sun, while direct observation of ammonia in radio wavelength region is more difficult by existed facilities. It is assumed that the fluorescence equilibrium is achieved and the collisional effect between molecules is negligible, which is reasonable because NH_2 exists mainly in outer part of coma where the gas density is sufficiently low for a typical comet. The model result shows that the (0,9,0) and (0,7,0) bands are suitable for comparisons between the observation and model results.

In Chapter 4, the first application of the fluorescence excitation model to the observations of two Oort cloud comets, comets C/1999S4 (LINEAR) and C/2001A2 (LINEAR), are shown. The OPRs of NH_2 are determined at the first time. The OPRs of 3.32 ± 0.09 and 3.43 ± 0.09 for NH_2 lead to OPRs of 1.16 ± 0.05 and 1.22 ± 0.05 for ammonia in comets C/1999S4 (LINEAR) and C/2001 (LINEAR), respectively. The derived spin tem-

peratures of ammonia were 28^{+3}_{-2} K and 26^{+2}_{-1} K. These results exclude the high-temperature limit and indicate the possible formation of ammonia through the grain related reactions. The ammonia formation in the icy mantle is supported by the present result. They corresponds to the formation region of the comets between the orbit of Saturn and that of Uranus in the solar nebula. It is consistent with the temperature ranges suggested by other observations of bright Oort cloud comets and consistent with the statistical studies based on the simulation of orbital evolution of comets. Further observations on other comets are required for investigating the formation region of comets, especially the comparison between Oort cloud and Kuiper belt comets is important for the study on evolution of our solar system.

Acknowledgments

I would like to thank Professor J. Watanabe at the National Astronomical Observatory of Japan (NAOJ) for a fruitful discussion and his continuous encouragement. Without his constant support, completion of this thesis project would have never been achieved.

I am also grateful to Professor S. Saito at the Fukui university for a valuable discussion and suggestions on the molecular spectroscopy. His many helpful suggestions encouraged me greatly.

I also wish to acknowledge Mr. O. Oshima, Dr. K. Ayani, and Mr. T. Kawabata at the Bisei Astronomical Observatory; Dr. H. Izumiura, and Dr. K. Yanagisawa at the Okayama Astrophysical Observatory; Dr. S. Masuda at the Kyoto university; Dr. W. Aoki at NAOJ and HDS members; Dr. T. Fuse, and Dr. T. Usuda at NAOJ, for their supports on the observations of comets.

I would like to acknowledge the staffs of the Gunma Astronomical Observatory for their supports.

NSO/Kitt Peak Fourier transform spectrometer data used here were produced by NSF/NOAO. This thesis is based on data collected at Subaru Telescope, which is operated by NAOJ.

Finally, I would like to express my appreciation to Dr. R. Furusho and my family for their continuous support and encouragement so far.

Bibliography

[1] Aikawa, Y., Ohashi, N., Inutsuka, S., Herbst, E., & Takakuwa, S., 2001, ApJ, 552, 639

[2] Aikawa, Y. & Herbst, E. 1999, ApJ 526, 314

[3] Aikawa, Y., Umebayashi, T., Nakano, T., Miyama, S. M. 1999, ApJ, 519, 705

[4] A'Hearn, M. F. 1978, ApJ, 219, 768

[5] A'Hearn, M. F. 1982, in *Comets*, Wilkening, L. L. & Matthews, M. S. Eds. (Univ. Arizona Press, Tucson, 1982), 433

[6] A'Hearn, M. F., Millis, R. L., Schleicher, D. G., Osip, D. J., & Birch, P. V. 1995, Icarus, 118, 223

[7] Amano, T., Bernath, P. F., & McKellar, A. R. W. 1982, J. Mol. Spectrosc., 94, 100

[8] Arpigny, C. 1994, AIP Conference Proceedings, 312, 205

[9] Bergin, E. A., Neufeld, D. A., Melnick, G. J. 1999, ApJ, 510, L145

[10] Biesner, J., Schnieder, L., Ahlers, G., Xie, Xiaoxiang, & Welge, K. H. 1989, J. Chem. Phy., 91, 2901

[11] Bird, M. K., Huchtmeier, W. K., Gensheimer, P., Wilson, T. L., Janardhan, P., & Lemme, C. 1997a, Astron.&Astrophy., 325, L5

[12] Bird, M. K., Janardhan, P., Wilson, T. L., Huchtmeier, W. K., Gensheimer, P., & Lemme, C. 1997b, Earth, Moon, and Planets, 78, 21

[13] Birss, F. W. & Ramsay, D. A. 1984, Comp. Phys. Comm. 38, 83

[14] Biver, N., Bockelée-Morvan, D., Crovisier, J., Davies, J. K., Matthews, H. E., Wink, J. E., Rauer, H., Colom, P., Dent, W. R. F., Despois, D., Moreno, R., Paubert, G., Jewitt, D., & Senay, M. 1999, AJ, 118, 1850

[15] Blake, G. A., Qi, C., Hogerheijde, M. R., Gurwell, M. A., & Muhleman, D. O. 1999, Nature, 398, 213

[16] Bockelée-Morvan, D., Lis, D. C., Wink, J. E., Despois, D., Crovisier, J., Bachiller, R., Benford, D. J., Biver, N., Colom, P., Davies, J. K., G rard, E., Germain, B., Houde, M., Mehringer, D., Moreno, R., Paubert, G., Phillips, T. G., & Rauer, H. 2000, Astron. &Astrophys., 353, 1101

[17] Bockelée-Morvan, D., Biver, N., Moreno, R., Colom, P., Crovisier, J., Gérard, É., Henry, F., Lis, D. C., Matthews, H., Weaver, H. A., Womack, M., & Festou, M. C. 2001, Science, 292, 1339

[18] Brown, J. M., Chalkley, S. W., & Wayne, F. D. 1979, Mol. Physics, 38, 1521 AJ, 112, 1197

[19] Brown, M. E., Bouchez, A. H., Spinrad, H., & Johns-Krull, C. M. 1996, AJ, 112, 1197

[20] Buenker, R. J., Peric, M., Peyerimhoff, S. D., & Marian, R. 1981, Mol. Physics, 43, 987

[21] Burkholder, J. B., Howard, C. J., & McKellar, A. R. W. 1988, J. Mol. Spectrosc., 127, 415

[22] Combi, M. R., & Delsemme, A. H. 1980, ApJ, 237, 633

[23] Combi, M. R., & Smyth, W. H. 1988, ApJ, 327, 1026

[24] Combi, M. R. & McCrosky, R. E. 1991, Icarus 91, 270

[25] Combi, M. R., Bos, B. J., & Smyth W. H. 1993, ApJ, 408, 668

[26] Combi, M. R., Disanti, M. A., & Fink, U. 1997a, Icarus, 130, 336

[27] Combi, M. R., Kabin, K., DeZeeuw, D. L., Gombosi, T. I., & Powell, K. G. 1997b, Earth, Moon, and Planets, 79, 275

[28] Cremonese, G. 1999, Space Science Reviews, 90, 83

[29] Crovisier, J. 1999, in *Formulation and Evolution of Solids in Space*, Greenberg, J.M. & Li A. Eds. (Kluwer Academic Pub., Netherlands, 1999), 389

[30] Crovisier, J., & Encrenaz, T. 2000, *COMET SCIENCE*, Cambridge univ. press.

[31] Crovisier, J., Biver, N., Moreno, R., Lis, D. C., Bockelée-Morvan, D., Womack, M., Colom, P., Henry, F., Lecacheux, A., Paubert, G., Despois, D., & Weaver, H. A. 2001, AAS, DPS meeting, 33, 43.06

[32] Dickens, J. E., & Irvine, W. M. 1999, ApJ, 518, 733

[33] Dressler, K. & Ramsay, D. A. 1959, Phil. Trans. Royal Soc. London. SerA, 251, 553

[34] Ermler, W. C., Hsieh, H. C., & Harding, L. B. 1988, Comp. Phys. Comm. 51, 257

[35] Farnham, T. L., Schleicher, D. G., Woodney, L. M., Birch, P. V., Eberhardy, C. A., & Levy, L. 2001, Science, 292, 1348

[36] Feldman, P. D., Fournier, K. B., Grinin, V. P., & Zvereva, A. M. 1993, ApJ, 404, 348

[37] Feldman, P. D., Weaver, H. A., & Burgh, E. B. 2001, AAS, DPS meeting, 33, 43.01

[38] Festou, M. 1981, Astron.&Astrophy., 95, 69

[39] Festou, M. C., Encrenaz, T., Boisson, C., Pedersen, H., & Tarenghi, M. 1987, Astron.&Astrophy., 174, 299

[40] Fink, U., & Hicks, M. D. 1996, ApJ, 459, 729

[41] Fink, U 1994, ApJ, 423, 461

[42] Fink, U., Combi, M.R., & DiSanti, M.A. 1991, ApJ, 383, 356

[43] Fujii, M. 2000, private communication

[44] Fuke, K., Yamada, H., Yoshida, Y., Kaya, K. 1988, J. Chem. Phys., 88, 5238

[45] Glinski, R.J., Post, E.A., & Anderson, C.M. 2001, ApJ, 550, 1131

[46] Goswami, J., & Vanhala, H. 2000, in *Protostars and Planets IV*, Mannings, V., Boss, A.P., & Russell, S.S. Eds. (Univ. Arizona Press, Tucson, 2000), 963

[47] Hadj Bachir, I., Huet, T. R., Destombes, J. L., & Vervloet, M. 1999, J. Mol. Spectrosc., 193, 326

[48] Hersant, F., Gautier, D., & Huré, J.-M. 2001, ApJ, 554, 391

[49] Herzberg, G. 1950, *Molecular Spectra and Molecular Structure, I. Spectra of Diatomic Molecules* (New York, Van Nostrand Renhold), 21

[50] Hiraoka, K., Yamashita, A., Yachi, Y., Aruga, K., & Sato, T. 1995, ApJ, 443, 363

[51] Ho, P. T. & Townes, C. H. 1983, Ann. Rev. Astron. Astrophys., 21, 239

[52] Hodges, R. R., Jr. 1990, Icarus, 83, 410

[53] Huebner, W. F., Keady, J. J., & Lyon, S. P. 1992, Astrophys. and Space Sci., 195, 7

[54] Huet, T. R., Hadj Bachir, I., Bolvin, H., Zellagui, A., Destombes, J. L., & Vervloet, M. 1996, Astron. &Astrophys., 311, 343

[55] Irvine, W. M. 1999, Space Science Reviews, 90, 203

[56] Irvine, W. M., Schloerb, F. P., Crovisier, J., Fegley,Jr., B., & Mumma, M. J., 2000, in *Protostars and Planets IV*, Mannings, V., Boss, A. P., & Russell, S. S. Eds. (Univ. Arizona Press, Tucson, 2000), 1159

[57] Jewitt, D. C., & Meech, K. J. 1986, ApJ, 310, 937

[58] Johns, J. W. C., Ramsay, D. A., Ross, S. C. 1976, Can. J. Phys., 54, 1804

[59] Jungen, Ch., Hallin, K.-E. J., Merer, A. J. 1980, Mol. Physics, 40, 25

[60] Kawakita, H. & Watanabe, J. 1998, ApJ, 495, 946

[61] Kawakita, H. & Fujii, M. 1998, ApJ, 502, L185

[62] Kawakita, H., Ayani, K., & Kawabata, T. 2000, Publ. Astron. Soc. Japan, 52, 925

[63] Kawakita, H., Watanabe, J., Kinoshita, D., Shinsuke, A., Furusho, R., Izumiura, H., Yanagisawa, K., & Masuda, S. 2001, Publ. Astron. Soc. Japan, 53, L5

[64] Krasnopolsky, V. A. & Tkachuk, A. 1991, AJ, 101, 1915

[65] Krasnopolsky, V. A. Mumma, M. J., Abbott, M., Flynn, B. C., Meech, K. J., Yeomans, D. K., Feldman, P. D., & Cosmovici, C. B. 1997, Science, 277, 1488

[66] Krasnopolsky, V. A. & Mumma, M. J. 2001, ApJ, 629

[67] Kurucz, R. L., Furenlid, I., Brault, J., & Testerman, L. 1984, National Solar Observatory Atlas No. 1

[68] Kurucz, R. L. 1992, Synthetic infrared spectra, in *Infrared Solar Physics*, IAU Symp. 154, Rabin, D. M. & Jefferies, J. T. Eds. (Kluwer Acad., Norwell, MA)

[69] Langer, W., van Dishoeck, E., Bergin, E., Blake, G. A., Tielens, A. G. G. M., Velusamy, T., & Whittet, D. C. B. 2000, in *Protostars and Planets IV*, Mannings, V., Boss, A. P., & Russell, S. S. Eds. (Univ. Arizona Press, Tucson, 2000), 29

[70] Lew H. 1976, Can. J. Phys. 54, 2028

[71] Longuet-Higgins, H. C. 1963, Mol. Physics, 6, 445

[72] Magee-Sauer, K., Scherb, F., Roesler, F. L., & Harlander, J. 1989, Icarus, 82, 50

[73] McKellar, A. R. W., Vervloet, M., Burkholder, J. B., & Howard, C.J. 1990, J. Mol. Spectrosc., 142, 319

[74] Marcy, G. W., Cochran, W. D., & Mayor, M. 2000, in *Protostars and Planets IV*, Mannings, V., Boss, A. P., & Russell, S. S. Eds. (Univ. Arizona Press, Tucson, 2000), 1285

[75] Meier, R., Eberhardt, P., Krankowsky, D., & Hodges, R. R. 1994, Astron. & Astrophys., 287, 268

[76] Meier, R., Owen, T. C., Matthews, H. E., Jewitt, D. C., Bockelée-Morvan, D., Biver, N., Crovisier, J., & Gautier, D. 1998a, Science, 279, 842

[77] Meier, R., Owen, T. C., Jewitt, D. C., Matthews, H. E., Senay, M., Biver, N., Bockelée-Morvan, D., Crovisier, J., & Gautier, D. 1998b, Science, 279, 1707

[78] Momose, T., Miki, M., Wakabayashi, T., Shida, T., Chan, M.-C., Lee, S. S., & Oka, T. 1997, J. Chem. Phys., 107, 7707

[79] Morrison, N. D., Knauth, D. C., Mulliss, C. L. & Lee, W. 1997, Publ. Astron. Soc. Pacific, 109, 676

[80] Mousis, O., Gautier, D., Bockelée-Morvan, D., Robert, F., Dubrulle, B., & Drouart, A. 2000, Icarus, 148, 513

[81] Müller, H. S. P., Klein, H., Bolov, S. P., Winnewisser, G., Morino, I., Yamada, K. M. T., & Saito, S. 1999, J. Mol. Spectrosc., 195, 177

[82] Mumma, M. J., Weaver, H. A., & Larson, H. P. 1987, Astron.&Astrophy., 187, 419

[83] Mumma, M. J., Weissman, P. R., & Stern, S. A. 1993, in *Protostars and Planets III*, Levy, E. H. & Lunine J. I. Eds. (Univ. Arizona Press, Tucson, 1993), 1177

[84] Mumma, M. J., DiSanti, M. A., Dellorusso, N., Xie, D. X., Fomenkova, M., & Magee-Sauer, K. 1996, IAU Circ. No.6366

[85] Mumma, M. J., Dello Russo, N., DiSanti, M. A., Magee-Sauer, K., Novak, R. E., Brittain, S., Rettig, T., McLean, I. S., Reuter, D. C., Xu, Li-H. 2001a, Science, 292, 1334

[86] Mumma, M. J., Dello Russo, N., DiSanti, M. A., Magee-Sauer, K., & Novak, R. 2001b, AAS, DPS meeting, 33, 46.05

[87] Noguchi, K., Ando, H., Izumiura, H., Kawanomoto, S., Tanaka, W., & Aoki, W. 1998, in proc. SPIE, 3355, 354

[88] Poynter, R. L. & Kakar, R. K. 1975, ApJ Suppl. Ser., 29, 87

[89] Press, W. H., Teukolsky, S. A., Vetterling, W. T., & Flannery, B. P. 1992, *Numerical Recipes in C*, 2nd ed. (Cambridge Univ. press, Cambridge)

[90] Quack, M. 1977, Mol. Physics, 34, 477

[91] Rauer, H., Arpigny, C., Boehnhardt, H., Colas, F., Crovisier, J., Jorda, L., Küppers, M., Manfroid, J., Rembor, K., & Thomas, N. 1997a, Science, 275, 1909

[92] Rauer, H., Arpigny, C., Boehnhardt, H., Colas, F., Crovisier, J., Jorda, L., Küppers, M., Manfroid, J., Rembor, K., & Thomas, N. 1997b, Science, 277, 1527

[93] Rohlfs, K. & Wilson, T. L. 1996, *Tools of Radio Astronomy*, 2nd ed., (Springer-Verlag, Berlin, Heidelberg)

[94] Ross, S. C., Birss, F. W., Vervloet, M., Ramsay, D. A. 1988, J. Mol. Spectrosc., 129, 436

[95] Saito, S., Ozeki, H., Ohishi, M., & Yamamoto, S. 2000, ApJ, 535, 227

[96] Sears, T.J. 1984, Computer Physics Reports 2, 1

[97] Sekiguchi, T., Yamamoto, T., Watanabe, J., Fukushima, H., Yamamoto, N., & Kinoshita, D. 1996, proceedings of the 29th ISAS Lunar and Planetary Symposium, 224

[98] Sekiguchi, T. 1997, private communication

[99] Shu, F. H., Adams, F. C., & Lizano, S. 1987, Ann. Rev. Astron. Astrophys., 25, 23

[100] Stern, S. A., Slater, D. C., Festou, M. C., Parker, J. W. M., Gladstone, G. R., A'Hearn, M. F., & Wilkinson, E. 2000, ApJ, 544, L169

[101] Stokes, G. H., Evans, J. B., Viggh, H. E. M., Shelly, F. C., Pearce, E. C. 2000, Icarus, 148, 21

[102] Suto, M., & Lee, L. C. 1983, J. Chem. Phys., 78, 4515

[103] Tegler, S. C. & Wyckoff, S. 1989, ApJ, 343, 445

[104] Tegler, S. C., Burke, L. F., Wyckoff, S., Womack, M., Fink, U., & DiSanti, M. 1992, ApJ, 384, 292

[105] Thekaekara, M. P. 1974, Applied Optics 13, 518

[106] Townes, C. H. & Schawlow, A. L. 1975, *Microwave spectroscopy* (Dover Publications)

[107] Trujillo, C. A. & Brown, M. E. 2001, ApJ, 554, L95

[108] Watanabe, J., & the SWAT Team 1996, proceedings of the 29th ISAS Lunar and Planetary Symposium, 212

[109] Weaver, H. A., Brooke, T. Y., Disanti, M. A., Mumma, M. J., Tokunaga, A., Chin, G., A'Hearn, M. F., Owen, T. C., & Lisse, C. M. 1997, AAS, DPS meeting 1997, 29, 34.05

[110] Weaver, H. A., Sekanina, Z., Toth, I., Delahodde, C. E., Hainaut, O. R., Lamy, P. L., Bauer, J. M., A'Hearn, M. F., Arpigny, C., Combi, M. R., Davies, J. K., Feldman, P. D., Festou, M. C., Hook, R., Jorda, L., Keesey, M. S. W., Lisse, C. M., Marsden, B. G., Meech, K. J., Tozzi, G. P., & West, R. 2001, Science, 292, 1329

[111] Weissman, P. R. 1999, Space Science Reviews, 90, 301

[112] Willacy, K., Klahr, H. H., Millar, T. J., & Henning, Th. 1998, Astron. &Astrophys., 338, 995

[113] Womack, M., Faith, D., Festou, M. C. Slater, D., & Stern, S. A. 1997, IAU Circ., 6542

[114] Wyckoff, S., Tegler, S. C., & Engel, L. 1991, ApJ, 368, 279

[115] Zhang, H. W., Zhao, G., & Hu, J. Y. 2001, Astron. &Astrophys., 367, 1049